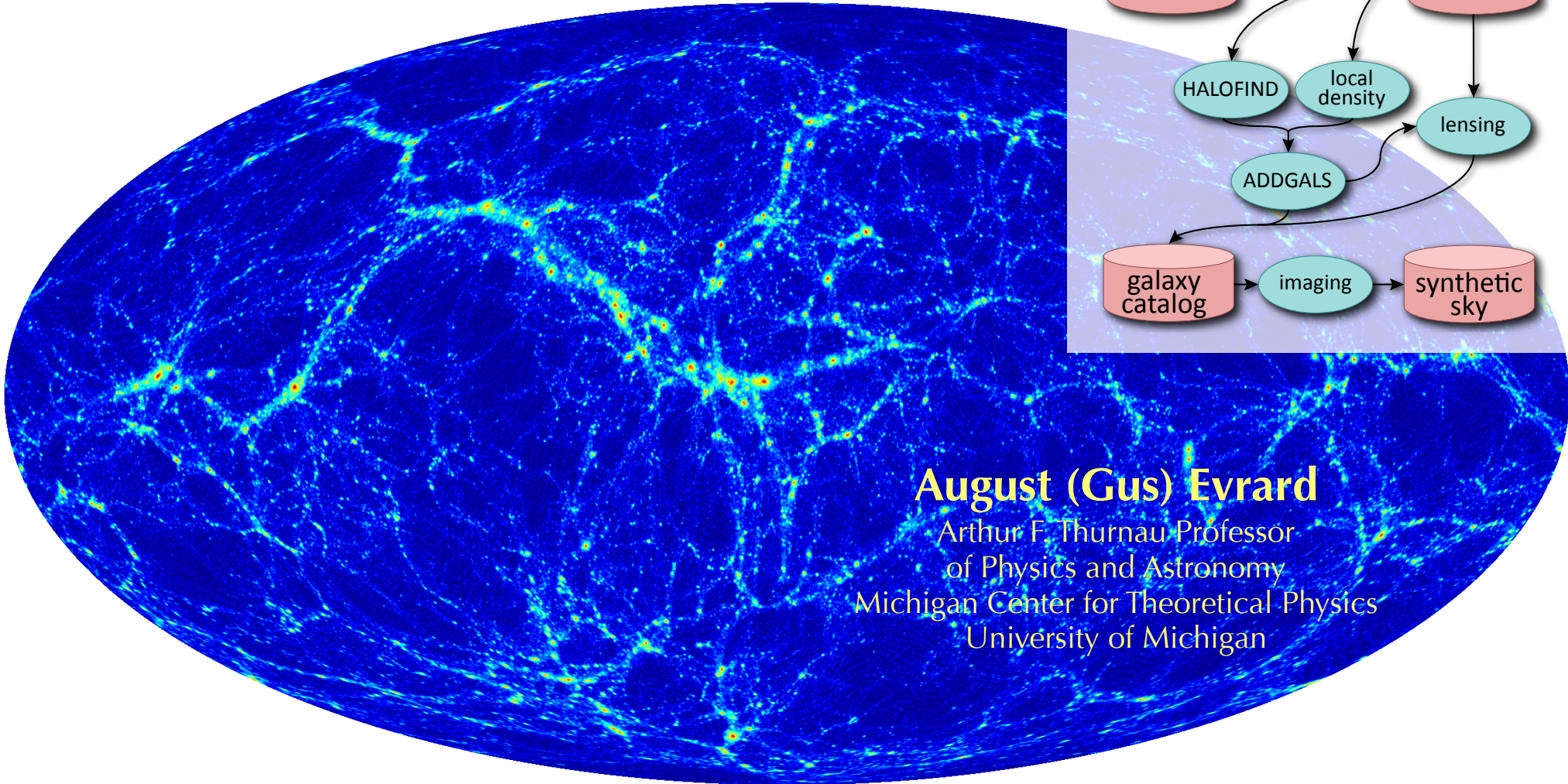
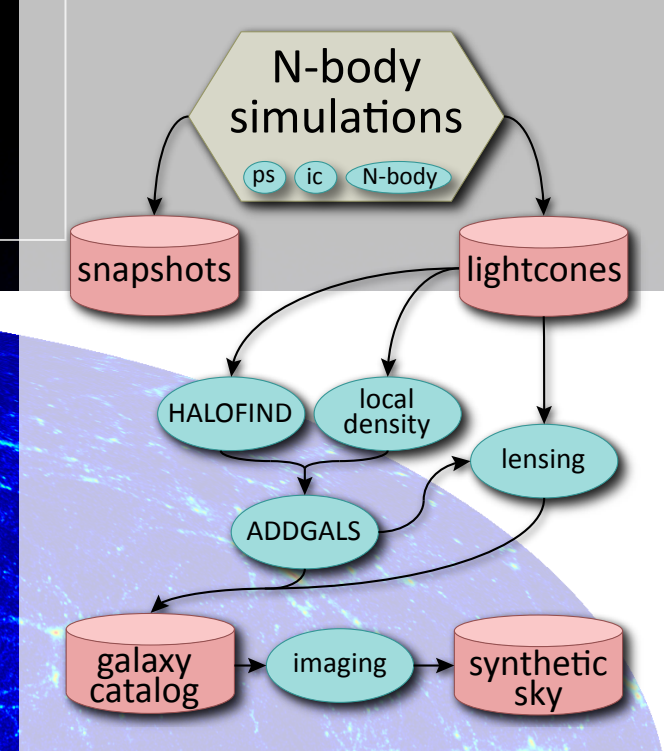


Simulations of Massive Halos: Past and Present (and toward the Future)



August (Gus) Evrard

Arthur F. Thurnau Professor
of Physics and Astronomy
Michigan Center for Theoretical Physics
University of Michigan

thread of the talk

- quick preamble...
- bias in hydrostatic mass estimates
 - implications for Planck maxBCG sample analysis
- the thorny physics of galaxy formation / cluster cores
 - a taste of new MHD results
- the less thorny issue of projection
 - a “quick halo sightline” generator
- synthetic sky production for Dark Energy Survey (DES)
 - 5,000 sq deg lensed galaxy catalogs under development
- closing thoughts
 - toward a simulation science gateway
haloHUB? Synthetic Cluster Observatory?

basic ingredients for cluster cosmology from counts + clustering

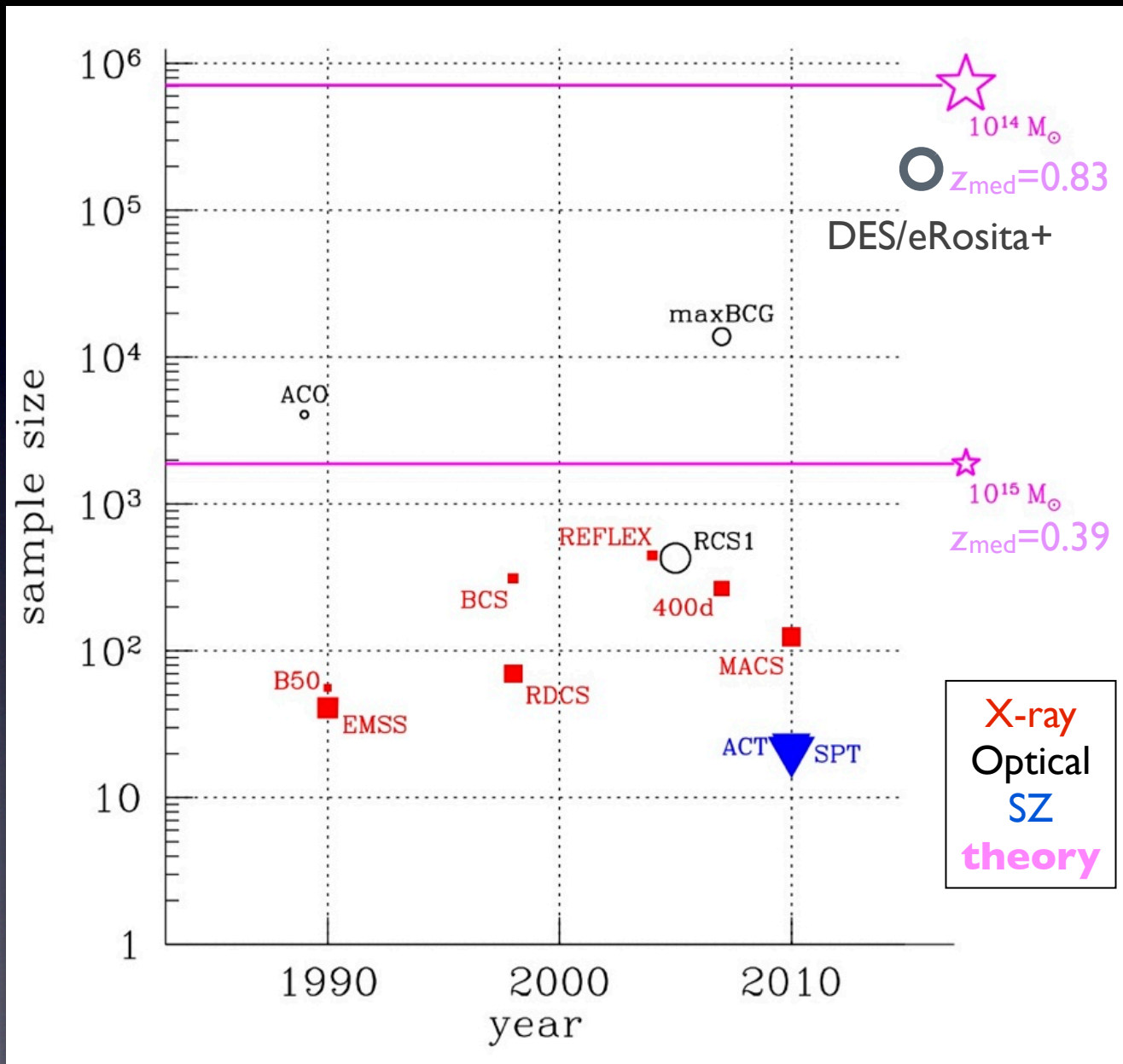
1. halo space density (aka, *mass function*), $dn(>M, z)/dV$
 - well calibrated ($\sim 5\%$ in dn) by (dark matter only) simulations
2. two-point spatial clustering of halos (aka, *bias function*), $b(M, z)$
 - similarly well calibrated
3. population model for signal, S , used to identify clusters, $p(S | M, z)$
 - power-law with log-normal deviations (typically self-calibrated)
 - projection effects (signal-dependent) $S_{\text{observed}} \neq S_{\text{intrinsic}}$
4. selection model for signal, S
 - completeness (missed clusters)
 - purity (false positives)

Briefly, the state of the art is:

Theory+simulations tell you how many halos are in the sky.

Observations tell you how to fill them with baryonic signatures.

cluster samples today are sparse relative to massive halos on the sky



Allen, Evrard & Mantz 2011

symbol size scales
with median redshift

Halo mass scale is
 M_{200m}
($h = 0.7$)

a prototypical 'relaxed' cluster

Allen, Evrard & Mantz 2011

Abell 1835 ($z=0.25$) seen in X-ray, optical and mm bands

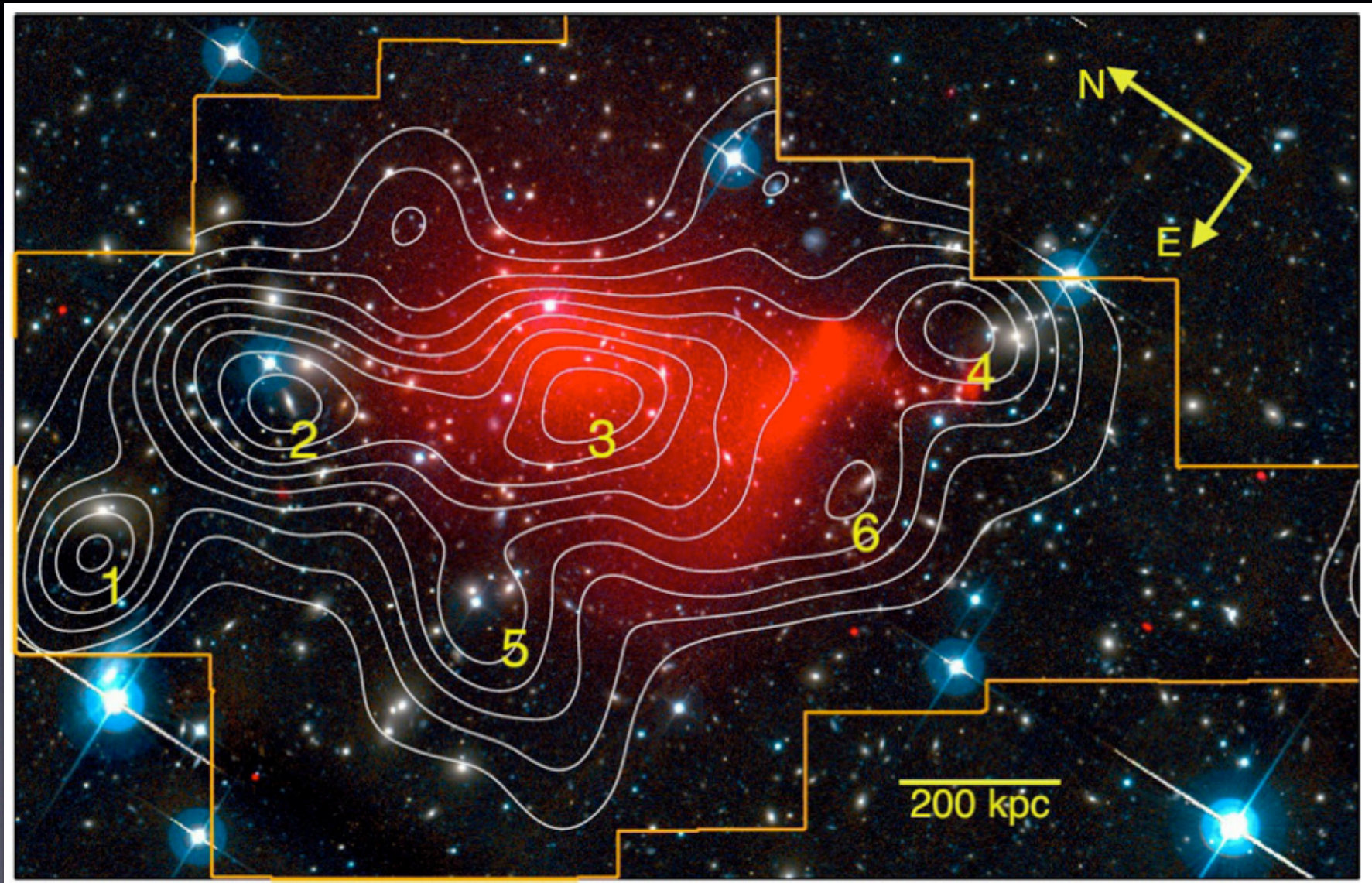


1.2 Mpc

an extreme `train wreck'

Jee et al 2012

Abell 520 ($z=0.20$) seen in **X-ray**, optical w/ lensing mass contours



cosmological complementarity from cluster counts + clustering

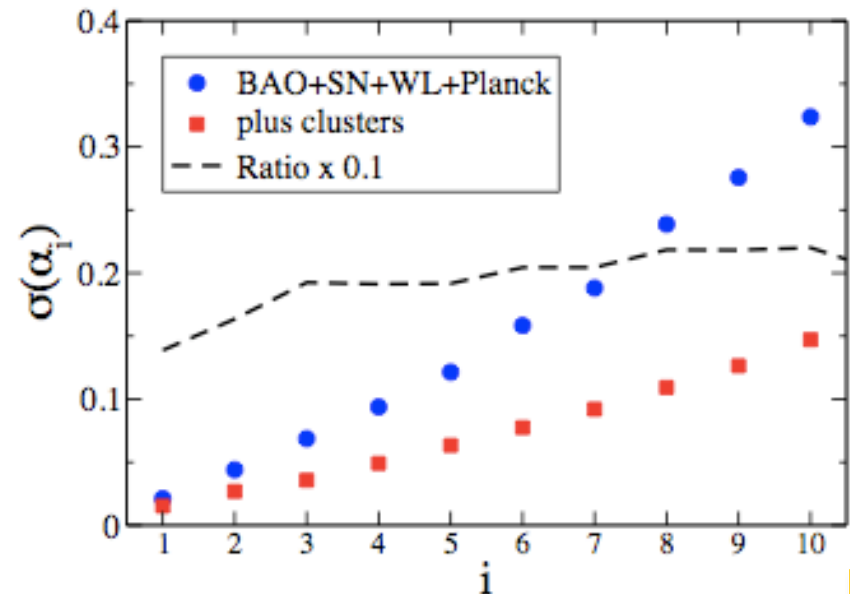
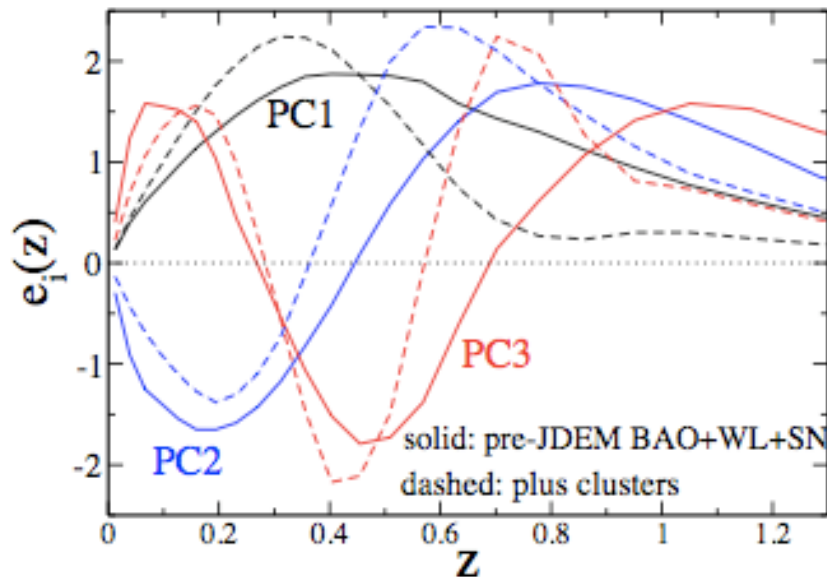
Cunha, Huterer, Frieman,
0904.1589

$$\ln M^{\text{bias}}(M_{\text{obs}}, z) = \ln M_0^{\text{bias}} + a_1 \ln(1+z) + a_2(\ln M_{\text{obs}} - \ln M_{\text{pivot}}) \quad (3)$$

$$\sigma_{\ln M}^2(M_{\text{obs}}, z) = \sigma_0^2 + \sum_{i=1}^3 b_i z^i + \sum_{i=1}^3 c_i (\ln M_{\text{obs}} - \ln M_{\text{pivot}})^i \quad (4)$$

← **nuisance:**
4 mass bias params
7 mass variance params

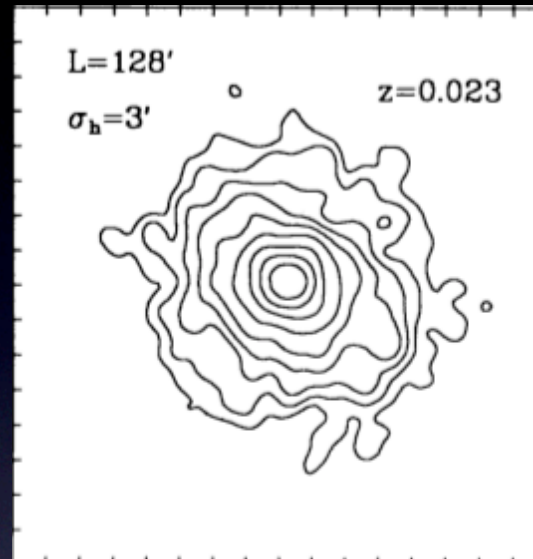
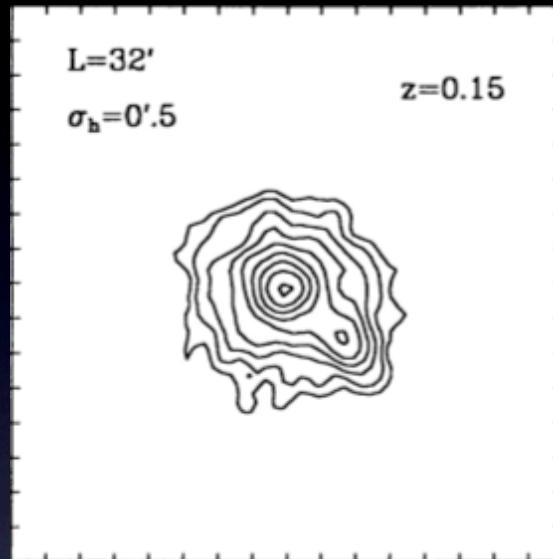
PCA analysis of DE figure of merit



X-ray based hydrostatic mass estimates

the deep, dark past of hydrostatic mass estimates from simulations

Evrard 1990



first application of
P3MSPH!

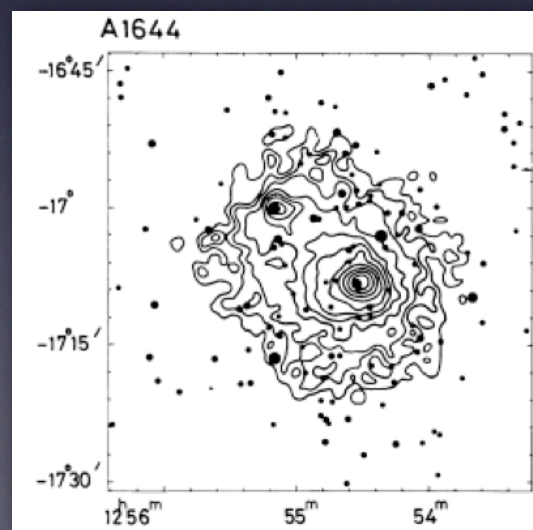
50 Mpc volume

'1989-standard-CDM'

$16^3 (=4096)$ particles

in each of DM + baryons

~ 500 particles/halo



Einstein image of A1644

Raychaudhury et al 1991

the deep, dark past of hydrostatic mass estimates from simulations

Evrard 1990

$$M_b(r) = 3\beta_g G^{-1} \frac{kT}{\mu m_p} r \frac{(r/r_{c,g})^2}{1 + (r/r_{c,g})^2}$$
$$= 1.1 \times 10^{14} \beta_g \frac{T}{\text{keV}} \frac{r}{\text{Mpc}} \frac{(r/r_{c,g})^2}{1 + (r/r_{c,g})^2} h_{50}^{-1} M_\odot. \quad (29)$$

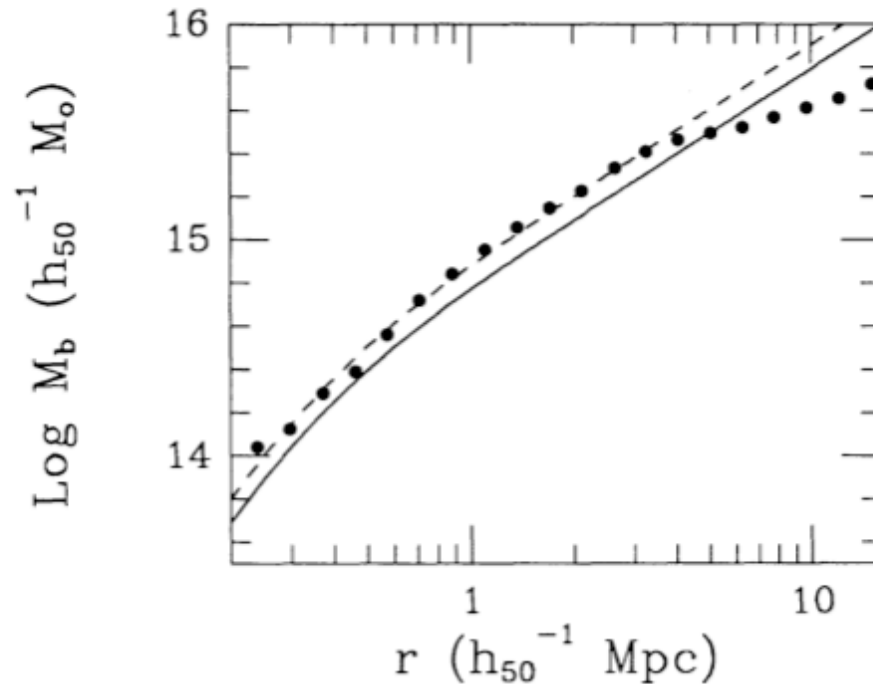


FIG. 12.—Binding mass predictions based on the hydrostatic, isothermal β -model compared to the actual enclosed mass profile (*filled circles*) of the model cluster at $z = 0$. The solid line is the uncorrected estimate given by eq. (29), while the dashed line shows this estimate corrected by a factor of 1.3.

Isothermal beta model mass estimates applied using 3D density and temperature profiles

Binding mass is underestimated by **30%** because of bulk gas motions - kinetic pressure, aka turbulence

still true in 2012...

ness. Clearly, more work needs to be done on resolving the important physical processes which compete to control the thermodynamics of the cluster core gas. Spherically symmetric

Evrard 1990
p. 365

see 2nd ICM Theory and Computation Workshop (2 weeks ago)

<http://www.umich.edu/~mctp/SciPrgPgs/events/2012/ICM/index.html>

recent hydrostatic mass bias from **ART** gas dynamic simulations

Lau et al (2011)

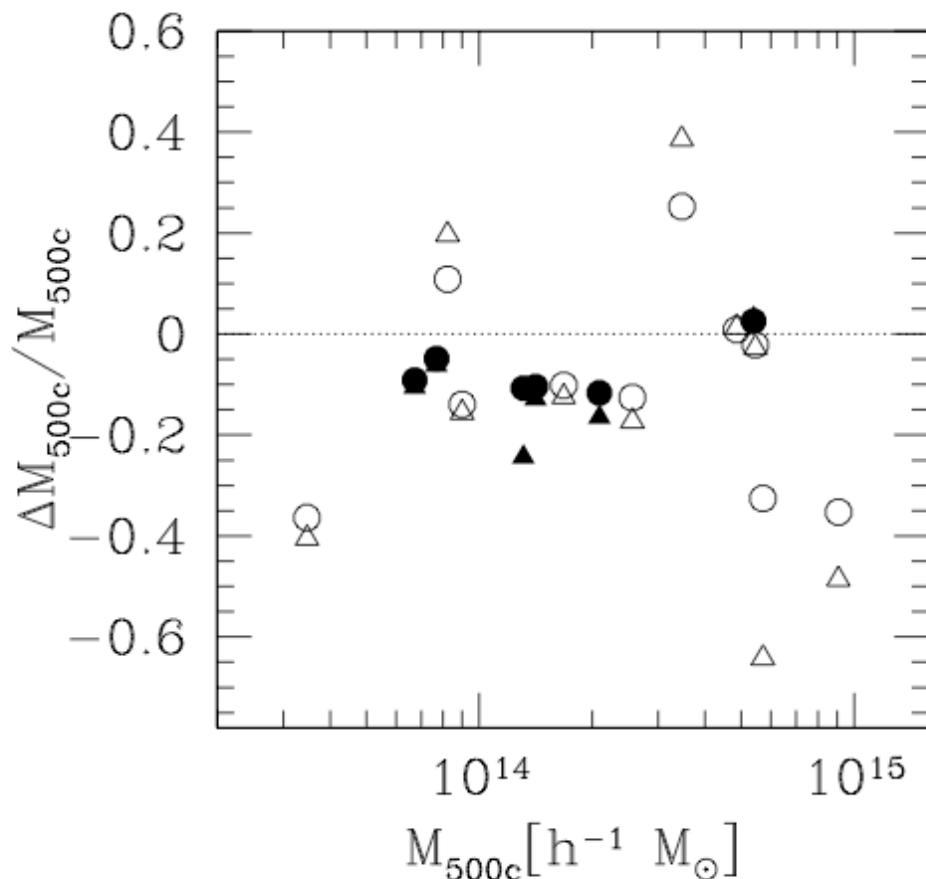


FIG. 6.— Fractional differences between the true mass and the HSE estimated mass, $\Delta M/M \equiv (M_{\text{est}} - M_{\text{true}})/M_{\text{true}}$, as a function of cluster mass M_{500c} . The circles and triangles show the hydrostatic mass evaluated at the true and estimated r_{500c} , respectively. The solid and open symbols indicate relaxed and unrelaxed clusters.

16 halos w/ cooling, star formation, SN feedback

~500,000 particles/halo

circles: true R_{500}

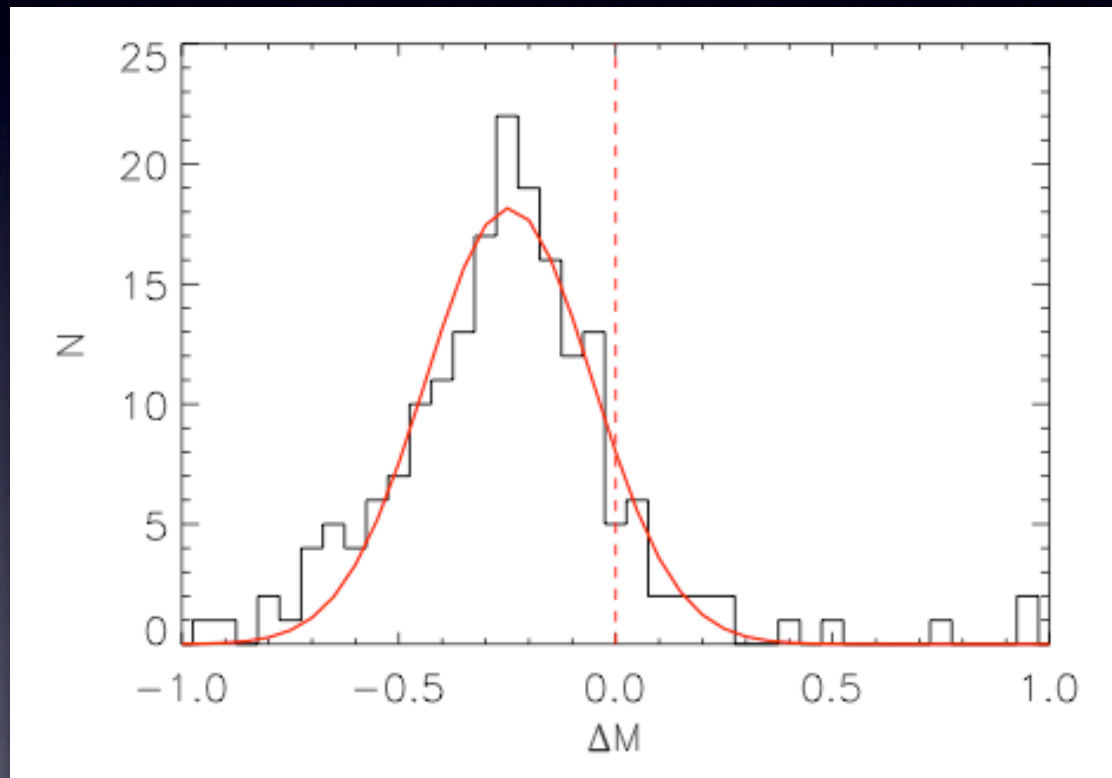
triangles: estimated R_{500}

difference = **aperture bias**

histogram of fractional errors

$$(M_{\text{HS}} - M_{\text{true}}) / M_{\text{true}}$$

using 3D information

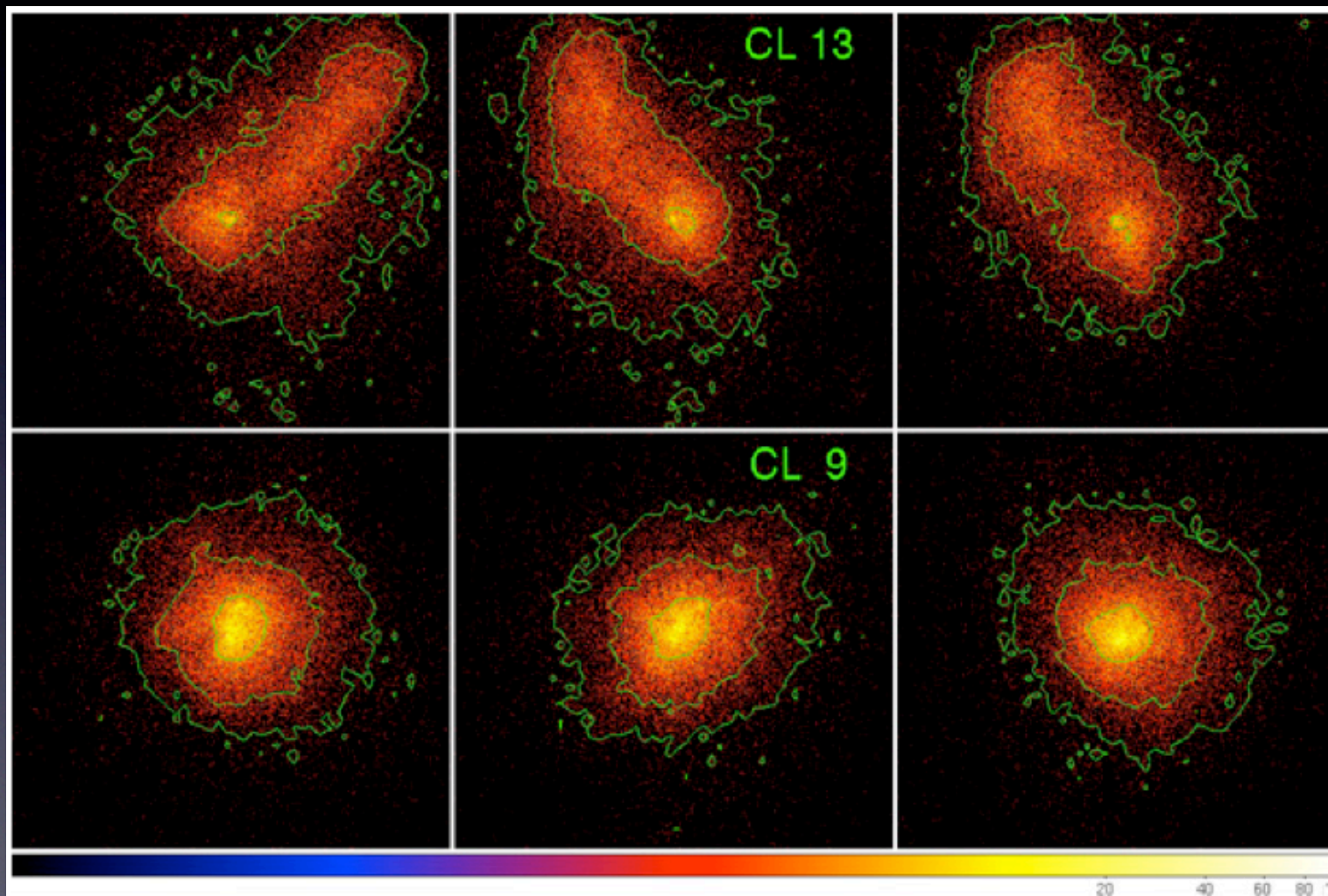


Marenostrum-MultiDark
Simulations (MUSIC)

- ~ 500 halos above $10^{14} M_{\text{sun}}$
modeled w/ CSF
- ~ 500,000 particles/halo

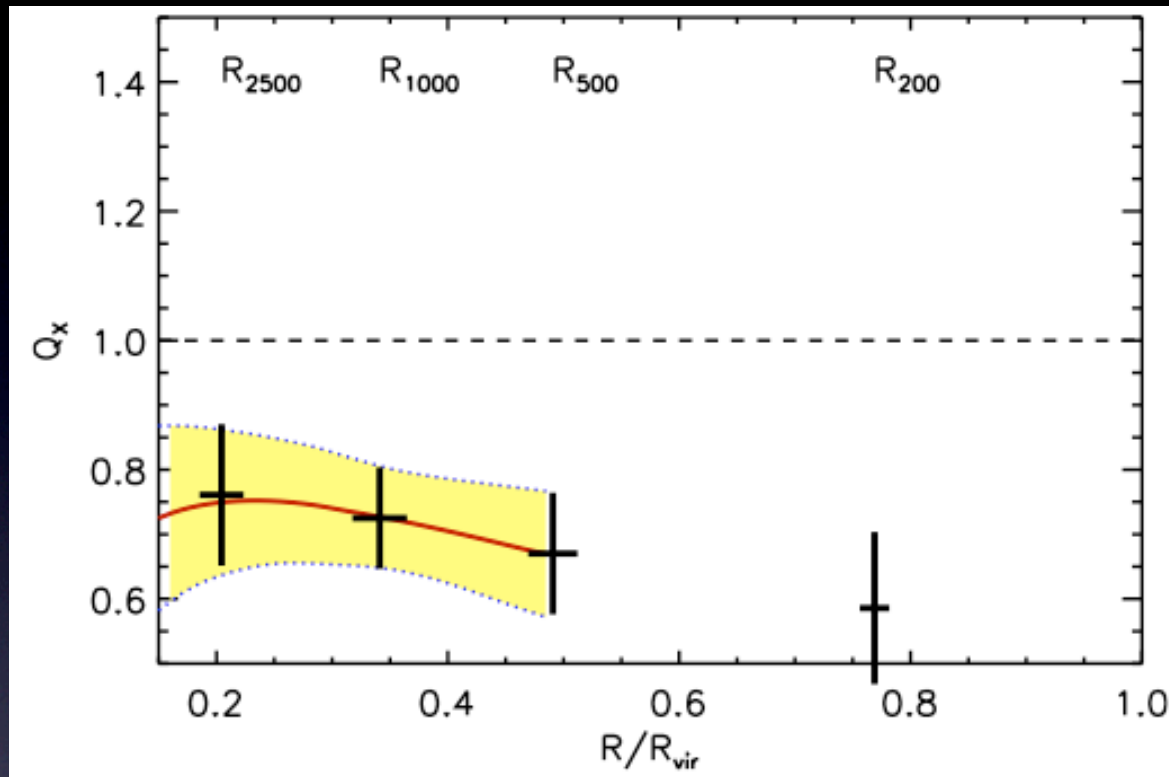
synthetic X-ray observations of Gadget simulations

Rasia et al (2012)



synthetic X-ray observations of Gadget simulations

Rasia et al (2012)



20 halos above $5 \times 10^{14} M_{sun}$
@ $z=0.25$

~ 500,000 particles/halo

ALL simulations studies show a **$20 \pm 5\%$ bias** underestimating total mass.

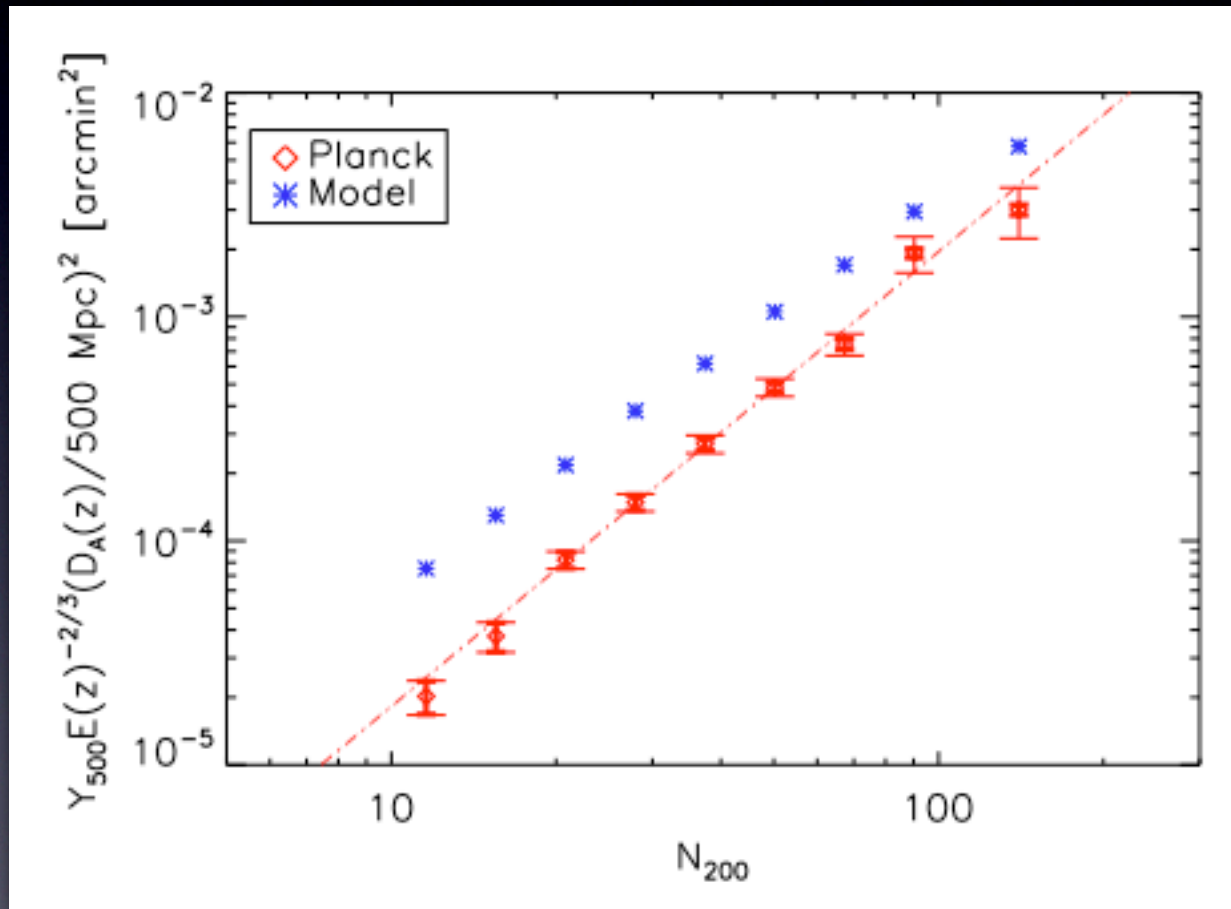
Due to the dynamic environment (mergers), the ICM in massive halos is not completely thermalized or perfectly hydrostatic.

Planck maxBCG sample: relieving the tension

with **Eduardo Rozo** + Eli Rykoff (Stanford)
+ Jim Bartlett (APC, Univ. Paris Diderot)

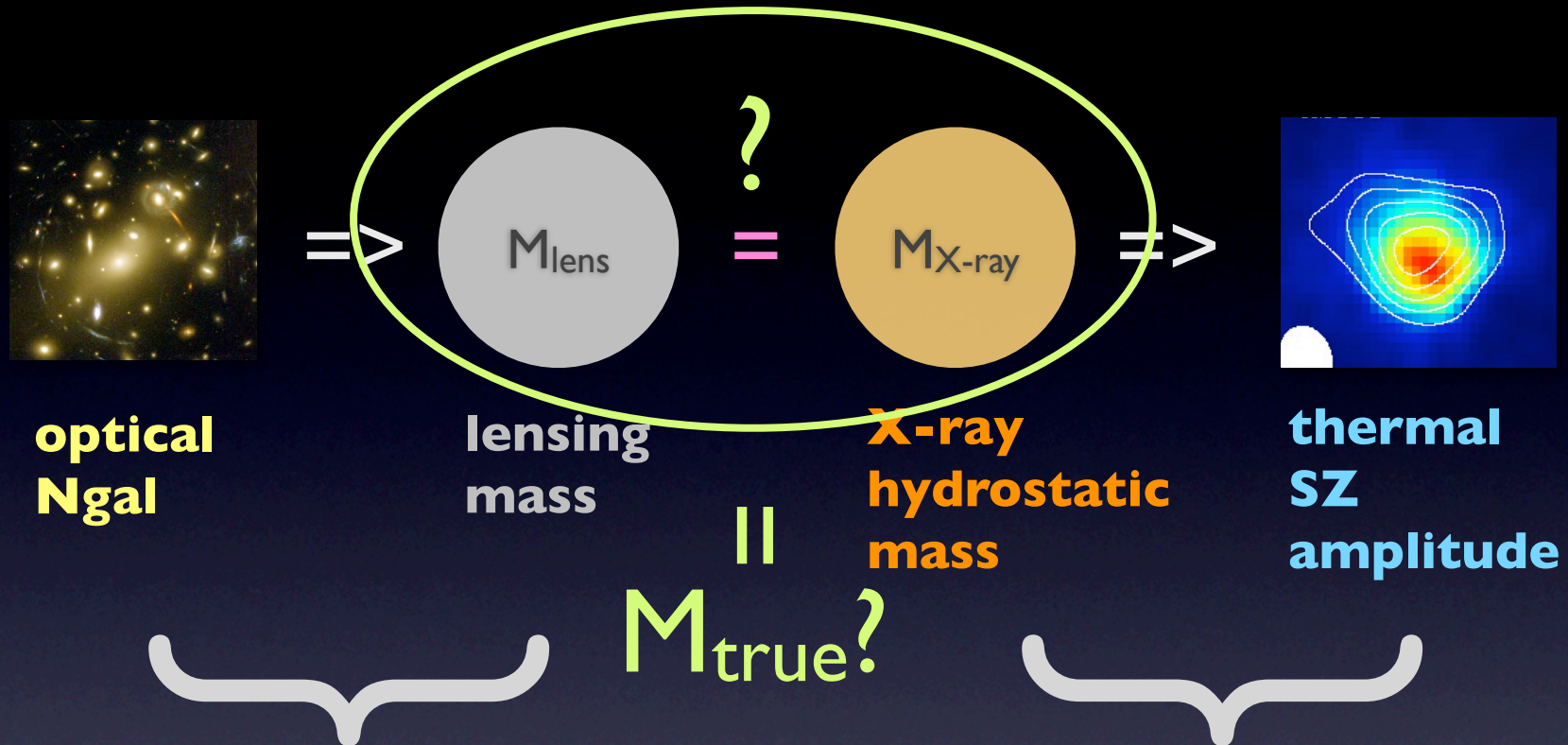
surprise from Planck stacking of optically-selected (maxBCG) clusters

Planck Collaboration arXiv:1101.2077



SZ decrement in maxBCG cluster sample is smaller than **model prediction** by factor >2

Planck model : steps from N_{gal} to Y_{sz}

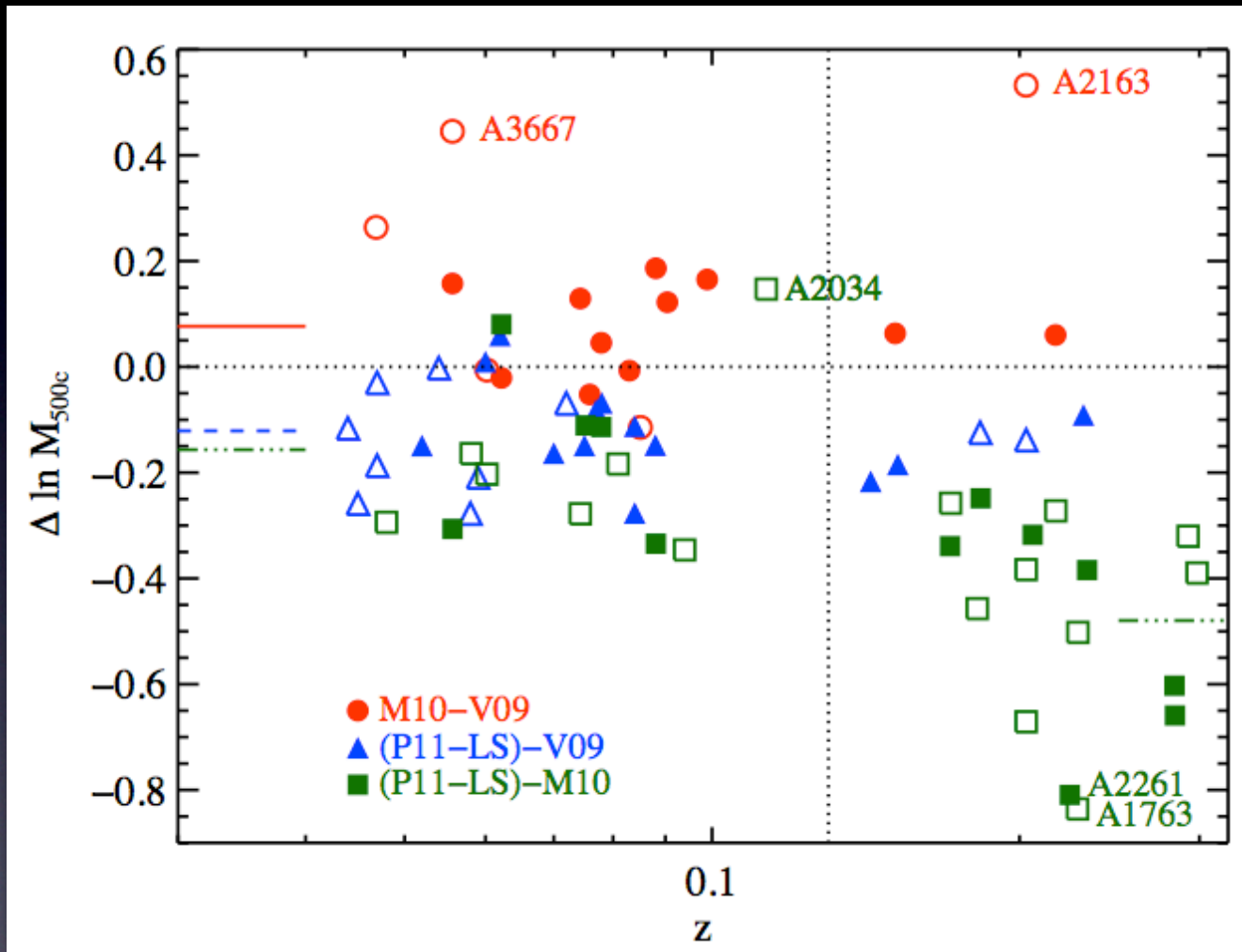


- * masses from stacked weak lensing analysis
- * optically-selected sample
- * based entirely on SDSS data

- * masses assume hydrostatic equilibrium of hot gas
- * X-ray selected samples
- * based mainly on XMM data
- * assumes $Y_x = Y_{sz}$
($Y_x = M_{gas} * T_x$)

comparison of published **total mass** (M_{500c}) estimates for local galaxy clusters

Rozo et al (2012) arXiv:1204.6301



y-axis shows
 $\ln(M_A / M_B)$
for samples A–B listed
in legend

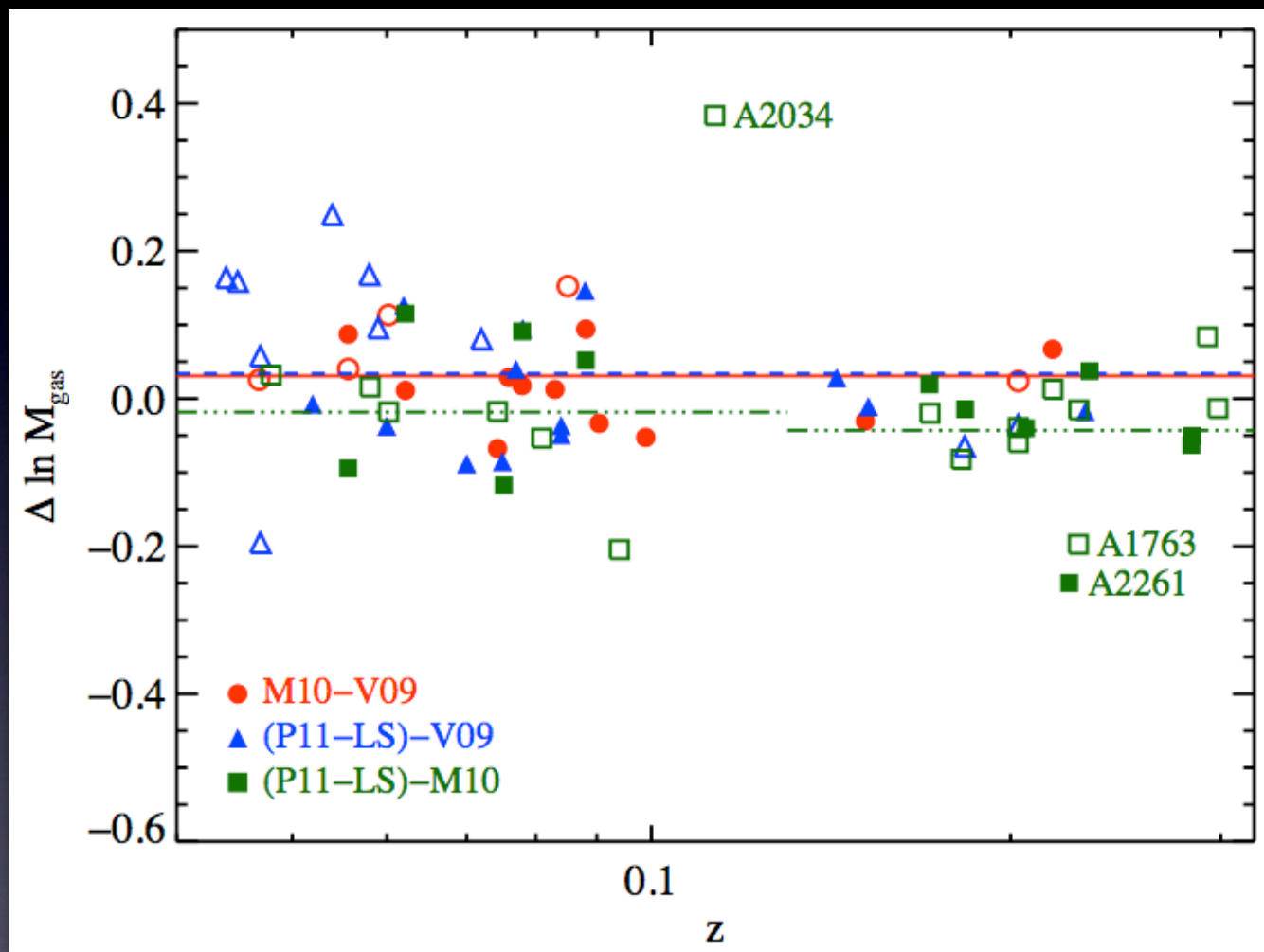
M10: Mantz et al (2010)
V09: Vihkinen et al (2009)
P11-LS: Planck Coll. (2011)

median published
statistical error $\sim 5\%$

filled: cool core/relaxed
open: non-cool core/unrelaxed

comparison of published **gas mass** estimates for local galaxy clusters

Rozo et al (2012) arXiv:1204.6301



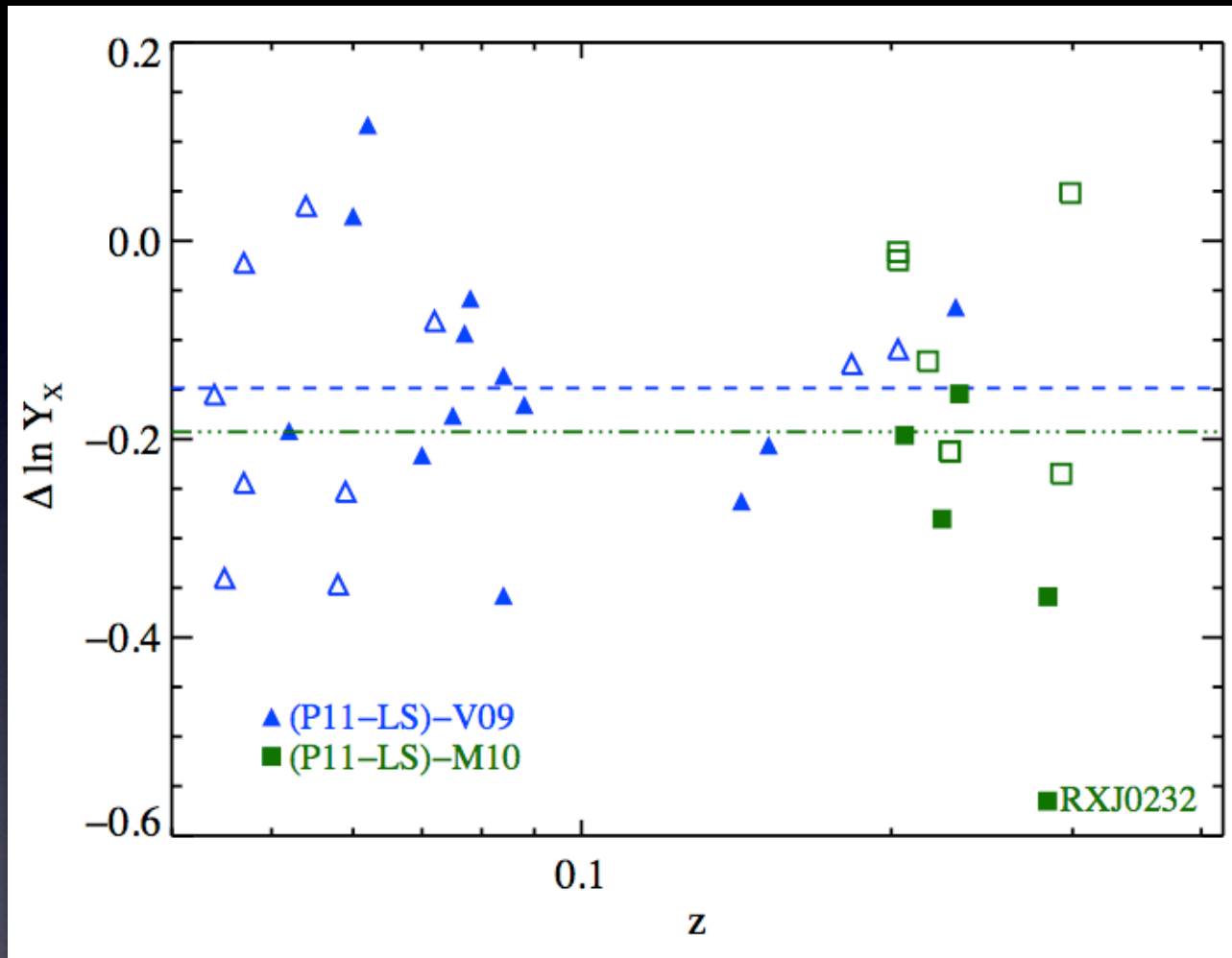
good agreement after
correcting to common
radial aperture

M10: Mantz et al (2010)
V09: Vihkinen et al (2009)
P11-LS: Planck Coll. (2011)

filled: cool core/relaxed
open: non-cool core/unrelaxed

comparison of published **gas thermal energy** estimates ($Y_x = M_{\text{gas}} * T_x$)

Rozo et al (2012) arXiv:1204.6301



fewer **independent** estimates of T_x (need long exposures)
=> no M10-V09

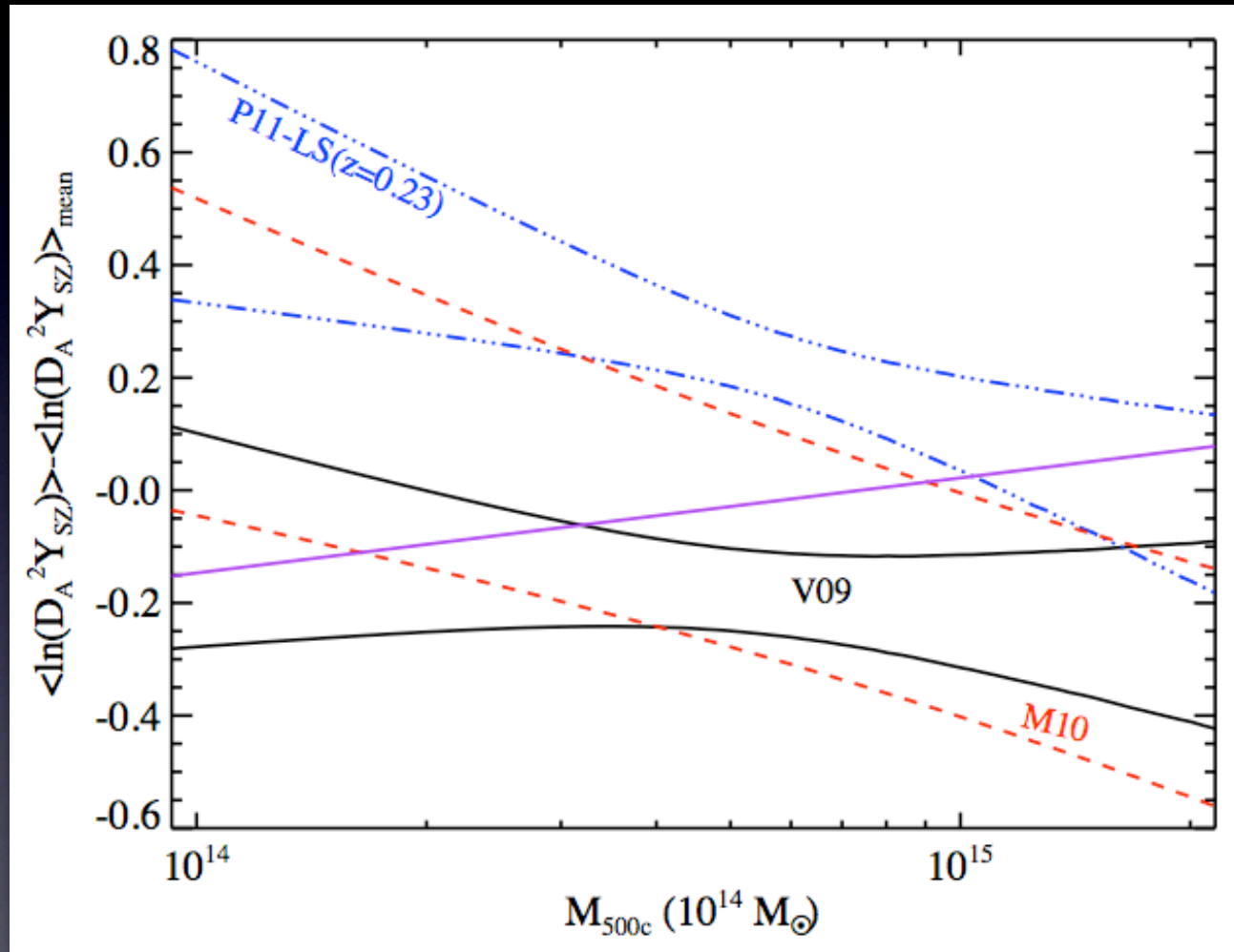
comparison is shown **after** correcting M_{gas} to common aperture

M10: Mantz et al (2010)
V09: Vihkinen et al (2009)
P11-LS: Planck Coll. (2011)

filled: cool core/relaxed
open: non-cool core/unrelaxed

Ysz-M scaling derived from power-law + log-normal covariance model

Rozo et al (2012) arXiv:1204.6292



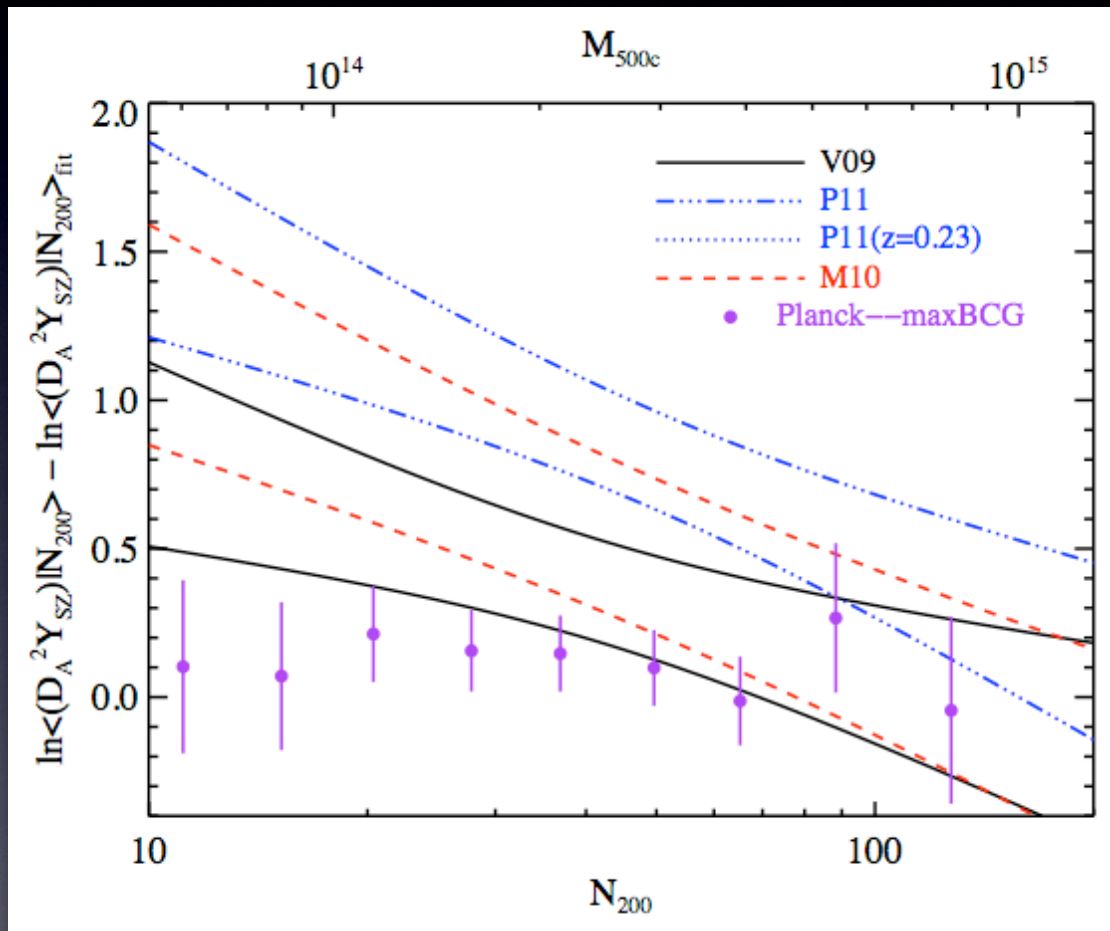
Use model to combine
published relations for
 $\langle M | Y_x \rangle$ and
 $\langle Y_{sz} | Y_x \rangle$
to derive
 $\langle Y_{sz} | M \rangle$

difference view using
reference w/ self-similar
slope (5/3) and mean
amplitude of 3 works

P11-LS ($z=0.23$) uses
 $Y_{sz}-Y_x$ for $0.13 < z < 0.3$
only (maxBCG z-range)
magenta line gives full
sample result

Ysz-N200 scalings : potential resolution

Rozo et al (2012) arXiv:1204.6305



Proposed resolution:

mass estimate biases
+ mis-centering

- 21% bias in hydrostatic masses (estimates are biased low)
- 10% reduction in maxBCG lensing masses measurements published in Rozo et al (2009) (~ 1 sigma systematic error)

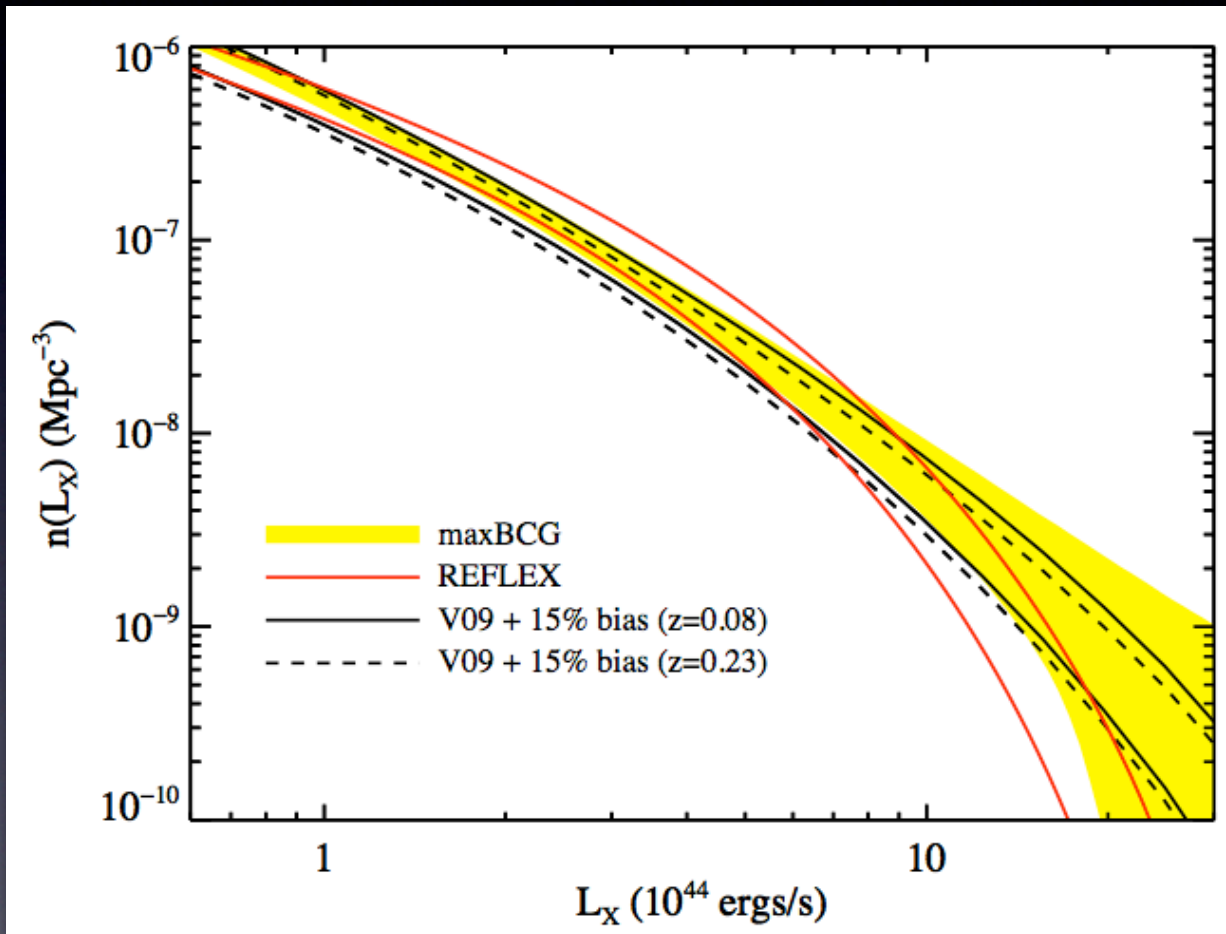
TABLE 4
PREFERRED SET OF SCALING RELATIONS

Relation	χ_0	Amplitude ($a_{\psi \chi}$)	$\alpha_{\psi \chi}$	$\sigma_{\ln \psi \chi}$	Sample
L_X-M	4.4	0.72 ± 0.07 (<i>ran</i>) ± 0.16 (<i>sys</i>)	1.55 ± 0.09	0.39 ± 0.03	V09+maxBCG
$D_A^2 Y_{SZ}-M$	4.4	0.87 ± 0.06 (<i>ran</i>) ± 0.17 (<i>sys</i>)	1.71 ± 0.08	0.15 ± 0.02	V09+maxBCG
$M-N_{200}$	40	0.75 ± 0.10	1.06 ± 0.11	0.45 ± 0.10	maxBCG
L_X-N_{200}	40	0.04 ± 0.10	1.63 ± 0.08	0.83 ± 0.10	maxBCG
$Y_{SZ}-N_{200}$	40	-0.24 ± 0.20	1.97 ± 0.10	0.70 ± 0.15	maxBCG
$Y_{SZ}-L_X$	1.0	-0.29 ± 0.06	1.10 ± 0.03	0.40 ± 0.05	P11-X

^a X-ray luminosity is measured in the [0.1, 2.4] keV band in units of 10^{44} ergs/s. $D_A^2 Y_{SZ}$ is in units of 10^{-5} Mpc². The maxBCG scaling relations are bias-corrected, while the V09+maxBCG relations are the joint constraint from the bias-corrected V09 and maxBCG samples. Scaling relations involving mass include a $\pm 10\%$ systematic uncertainty in the mass. The error in the amplitude of the $Y_{SZ}-L_X$ relation is larger than that quoted in P11-X because we include the uncertainty in our systematic corrections. This set of scaling relations is fully self-consistent.

abundance test of preferred scalings

Rozo et al (2012) arXiv:1204.6305



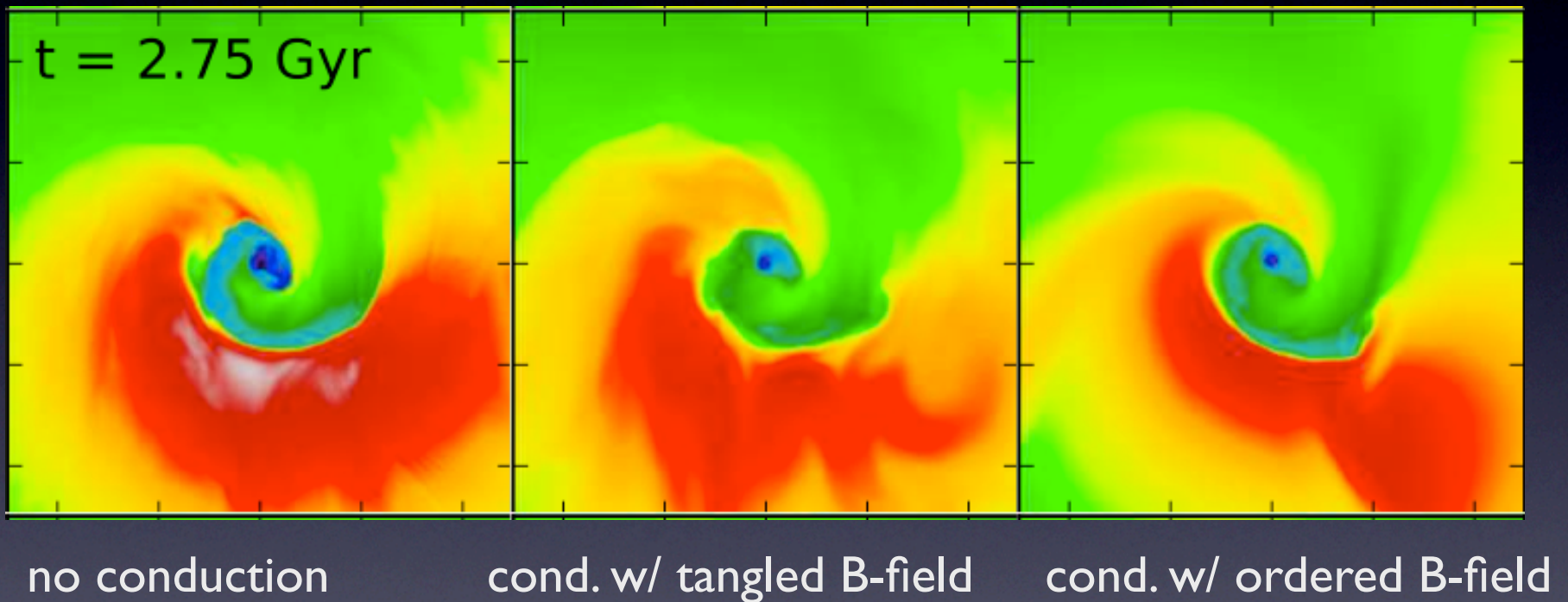
consistency check:

- maxBCG number counts convolved with L_X -N200 relation
- halo mass function convolved with V09 (adjusted) L_X -M relation
- compare to REFLEX luminosity function

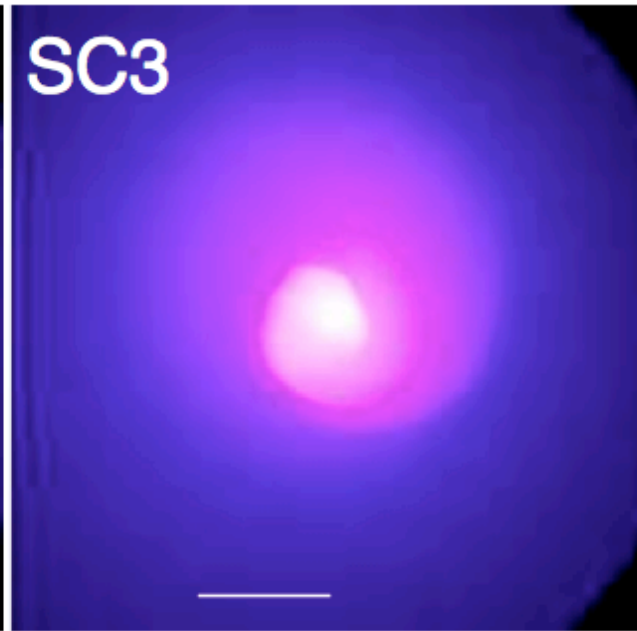
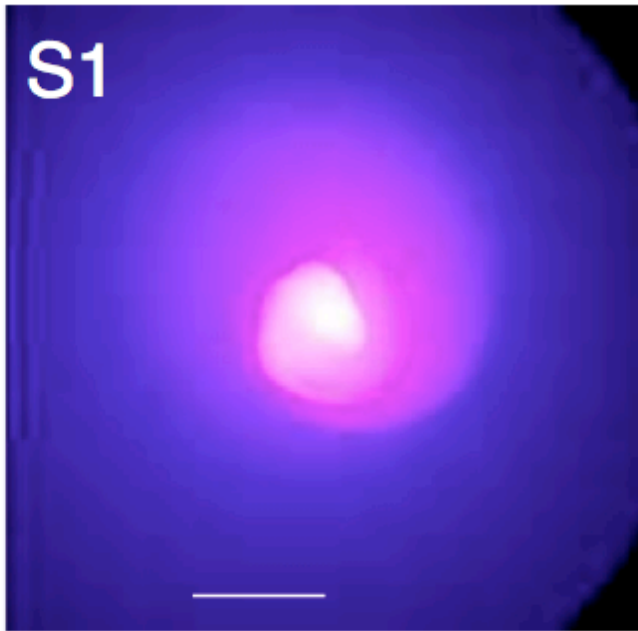
thorny physics of galaxy formation / cluster cores

2 highlights from 2nd Michigan ICM Theory and Computation Workshop
w/ Mateusz Ruskowski

FLASH sims: ideal MHD, anisotropic conduction
w/ radiative cooling



no
cond.



cond.
0.1
Spitzer

cond.
full
Spitzer

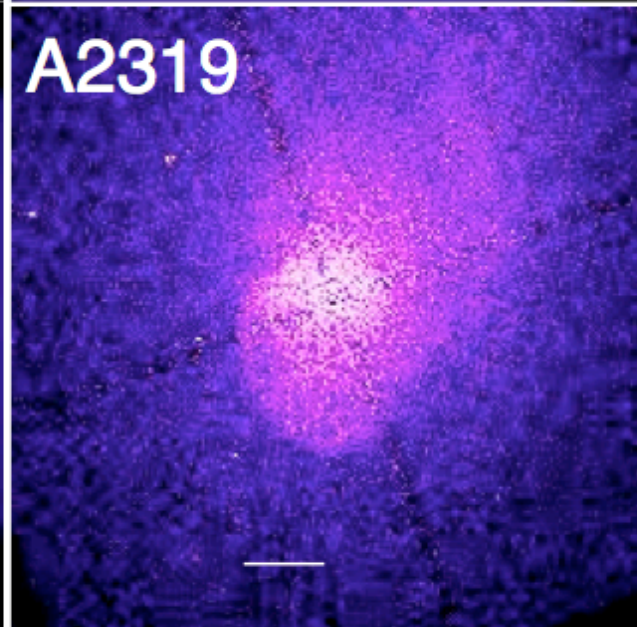
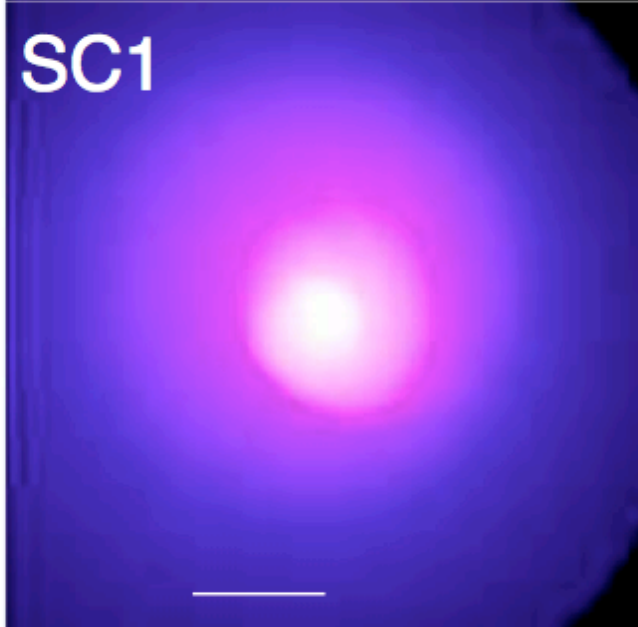


FIG. 7.— Projected X-ray emission along the z -axis of the simulation domain for the *S1* (no conduction), *SC1* (Spitzer conduction), and *SC3* (0.1 Spitzer conduction) simulations at the epoch $t = 2.75$ Gyr, with a *Chandra* X-ray image of A2319 included for comparison. White

2D sims w/
ATHENA
code

Magnetically aligned cold filaments are then able to form by local thermal instability. Viscous dissipation during cold filament formation produces accompanying hot filaments, which can be searched for in deep *Chandra* observations of cool-core clusters.



1990 all over again...

Despite such progress, there are still a number of unanswered questions, some of which may be addressed by well-resolved global, 3D numerical simulations of cluster cool cores and cluster outskirts. However, the efficacy of such simulations is likely to be contingent upon the implementation of a realistic sub-grid model for the microscale instabilities that captures their interplay with the computationally resolved meso- and macroscales. While formulating such a model is a rather formidable task, dedicated efforts to construct a more complete microphysical theory and to understand its bearing on heat and momentum transport, magnetogenesis, and thermodynamic stability in astrophysical systems are clearly needed.

Kunz et al 2012

a “quick halo sightline” approach to modeling projection

with Anbo Chen (UMich)

observed signal from a cluster is a sum of intrinsic + projected pieces

Chen & Evrard, in prep.

$$\begin{aligned} S_{\text{obs}}(m_t, z_t) &= S_{\text{int}}(m_t, z_t) + S_{\text{proj}}(m_t, z_t) \\ &= S_{\text{int}}(m_t, z_t) + \sum_i \Delta S(m_i, z_i, \Delta\theta_i | m_t, z_t), \end{aligned}$$

Observed signal within θ_{200} is sum of intrinsic + projection

$$\begin{aligned} p_{\text{proj}}(m, z, \Delta\theta | m_t, z_t) \\ &= p_{\text{ran}}(m, z) + p_{\text{cor}}(m, z, \Delta\theta | m_t, z_t) \\ &\propto n(m, z) + n(m, z) \xi_{hh}(m, z, \Delta\theta | m_t, z_t), \end{aligned}$$

Projected component is random + correlated halos along a given “target halo” sight-line

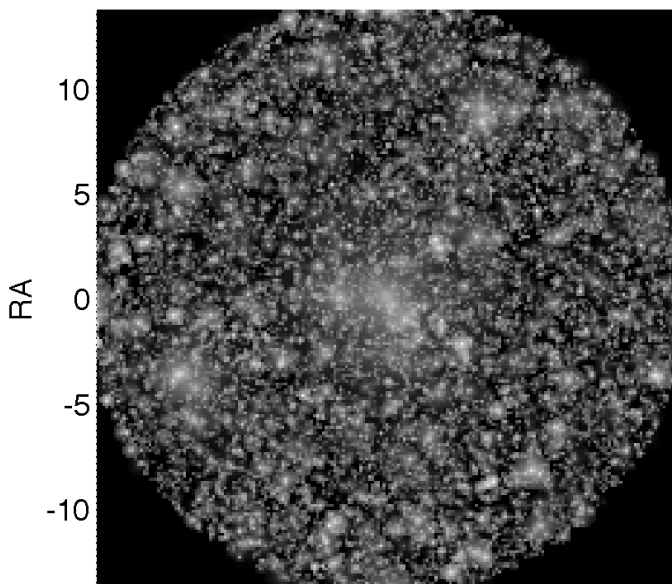
Signals:

optical : power-law $N_{\text{gal}}(M, z)$ with Poisson scatter

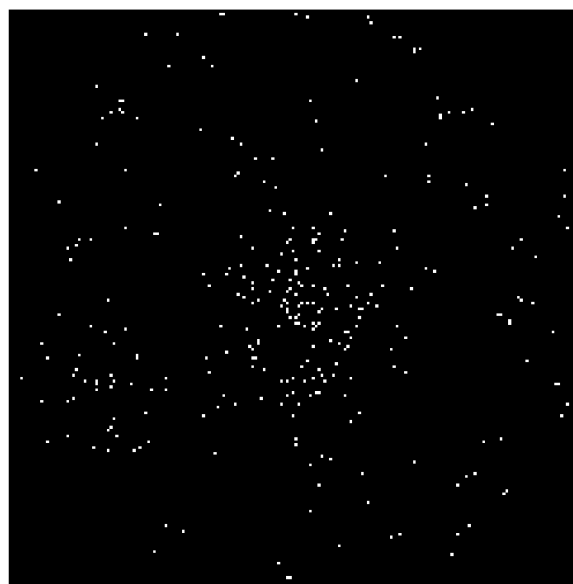
SZ : weakly curved power-law $Y(M, z)$ with log-normal scatter

X-ray : weakly curved power-law $L_X(M, z)$ with log-normal scatter

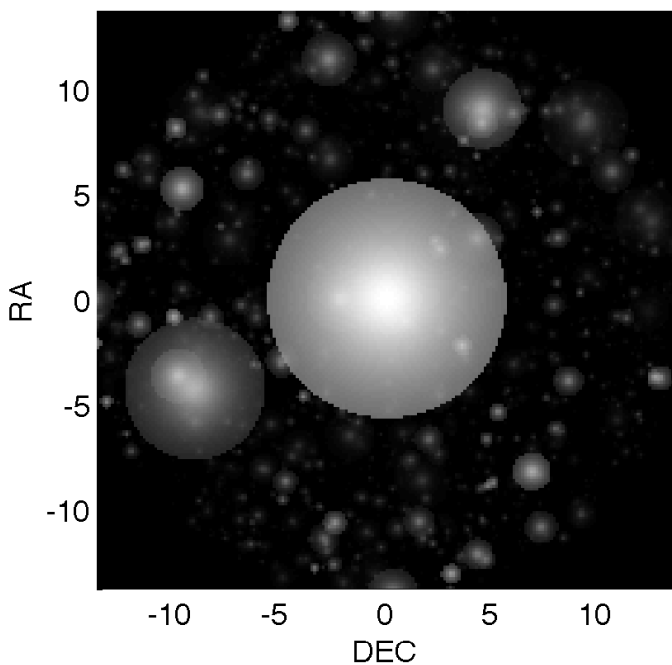
surface
mass
density



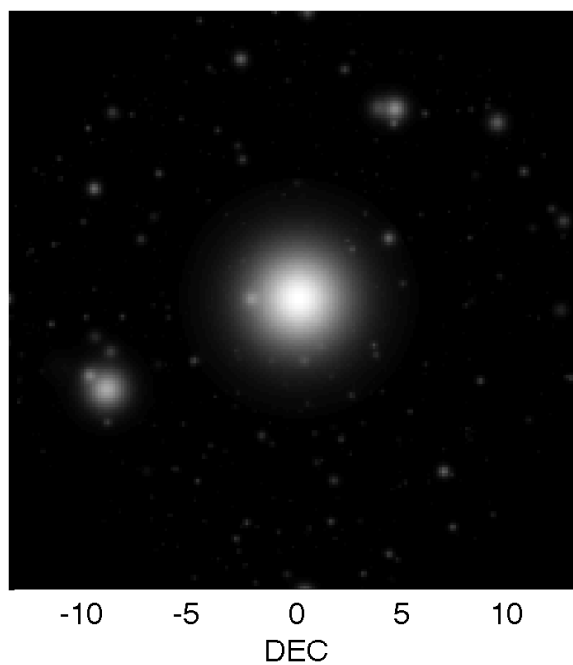
red-
sequence
galaxies



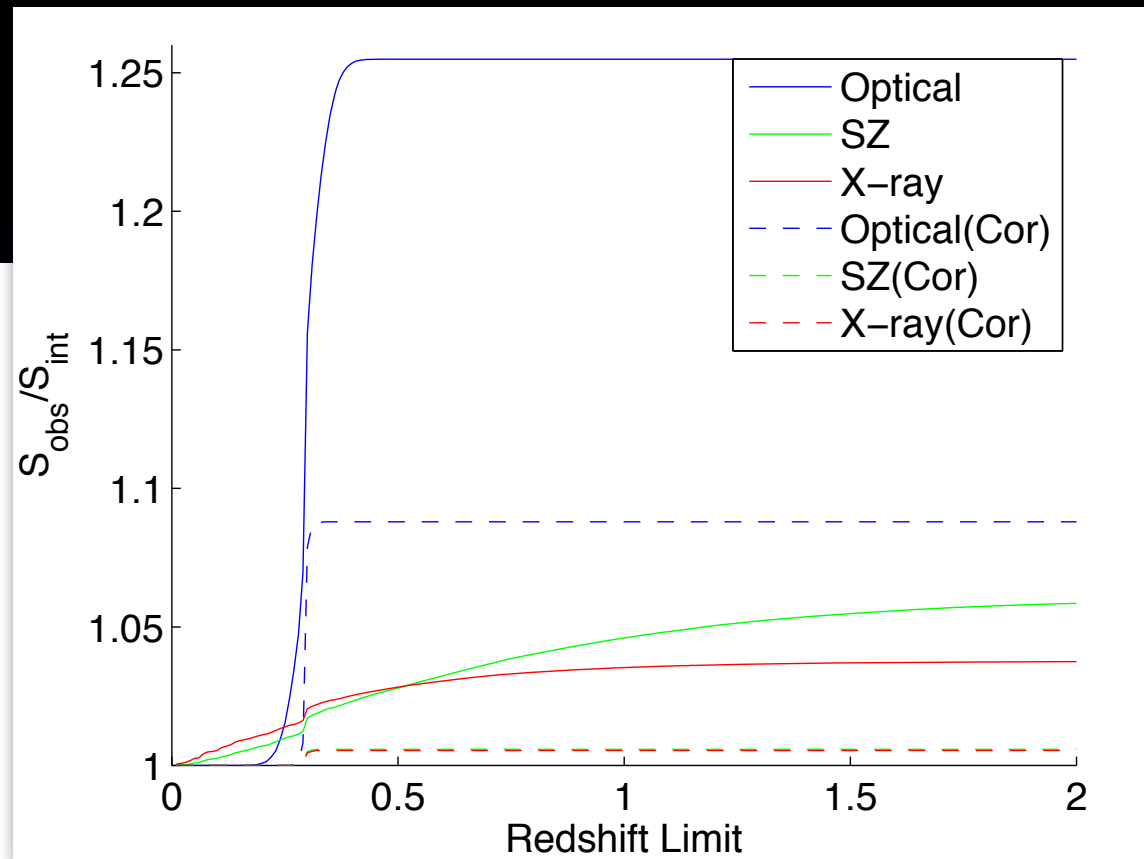
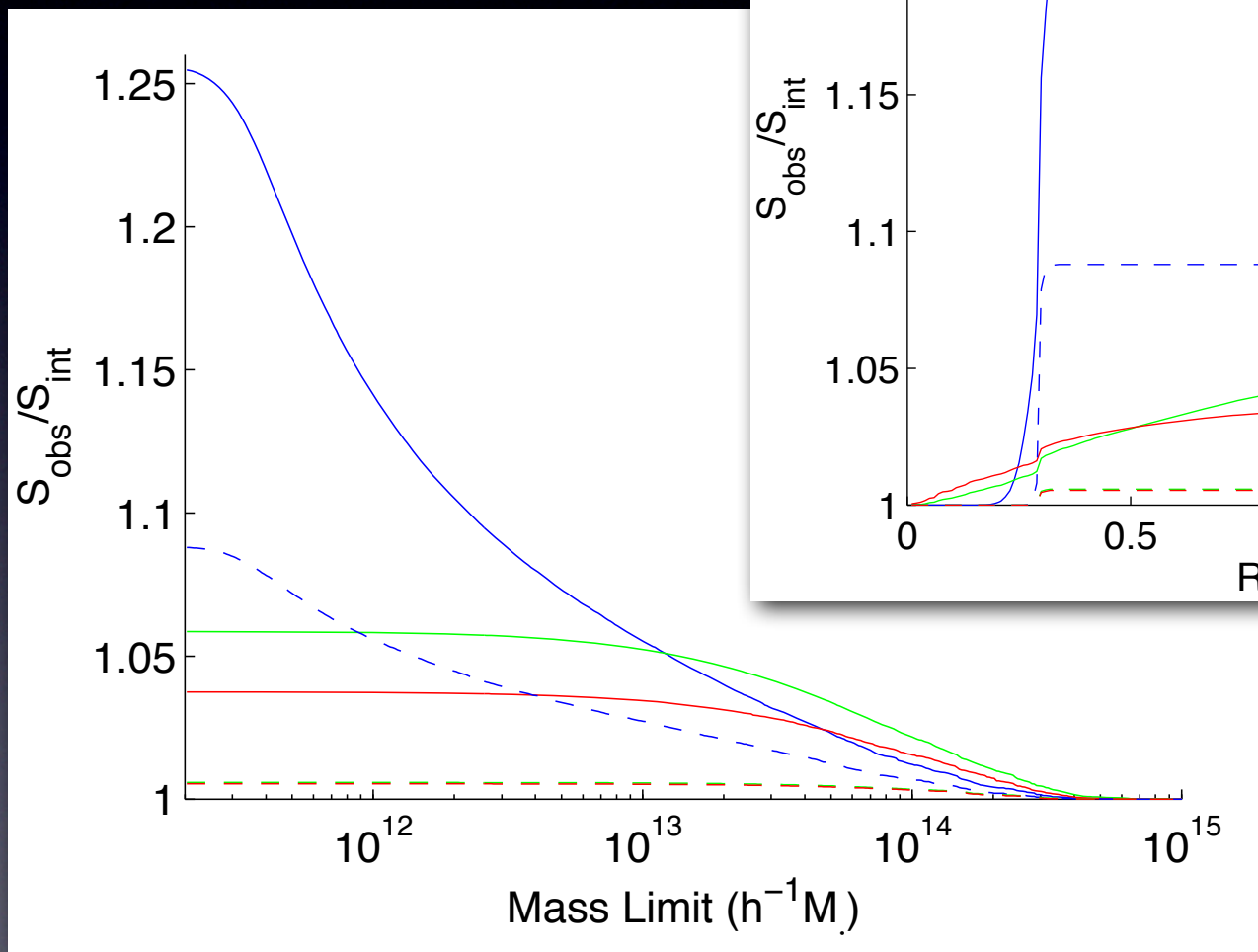
thermal
SZ
effect



X-ray
surface
brightness

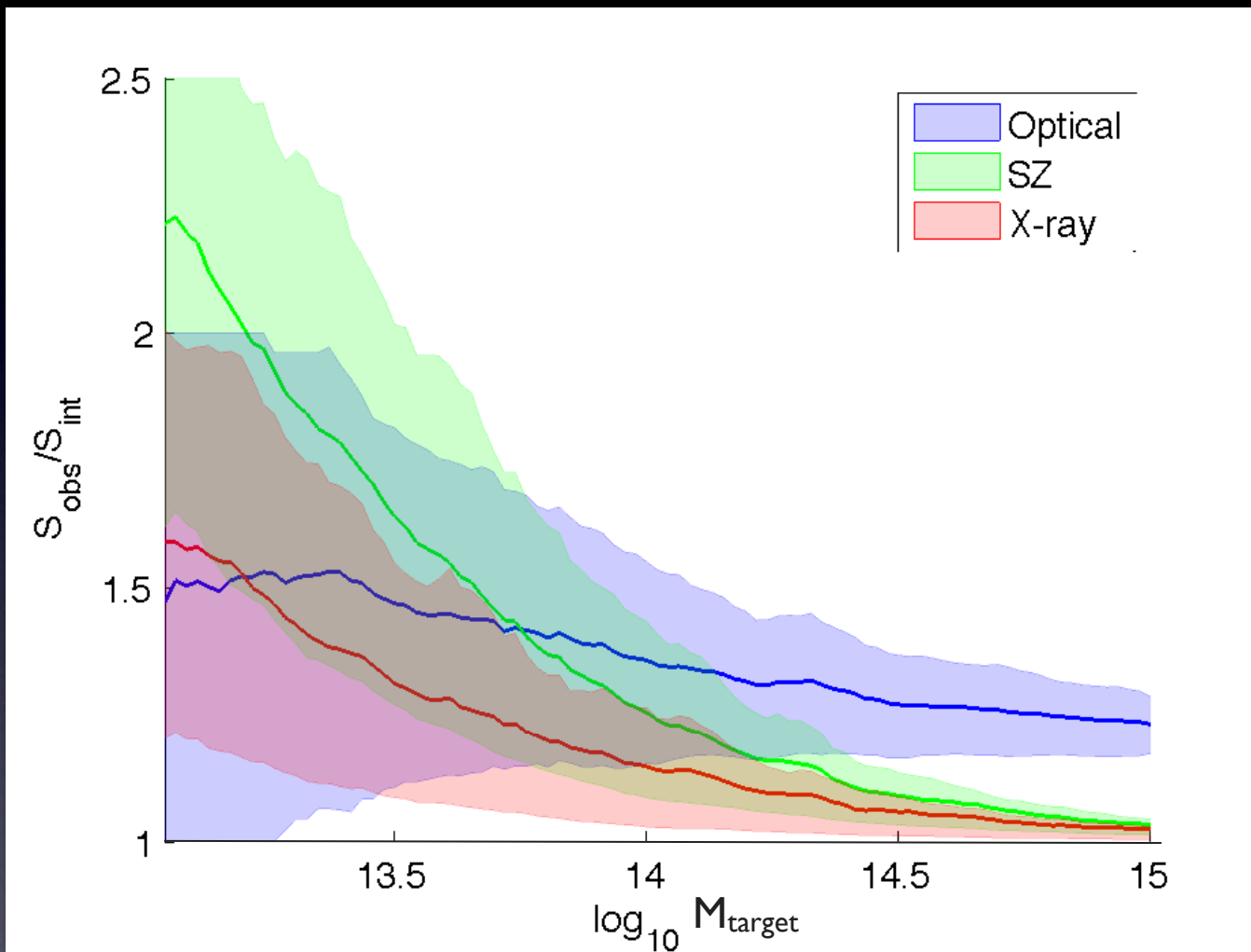


target: $\log(M_t)=14.5, z_t=0.3$



redshift limit of
projected halos

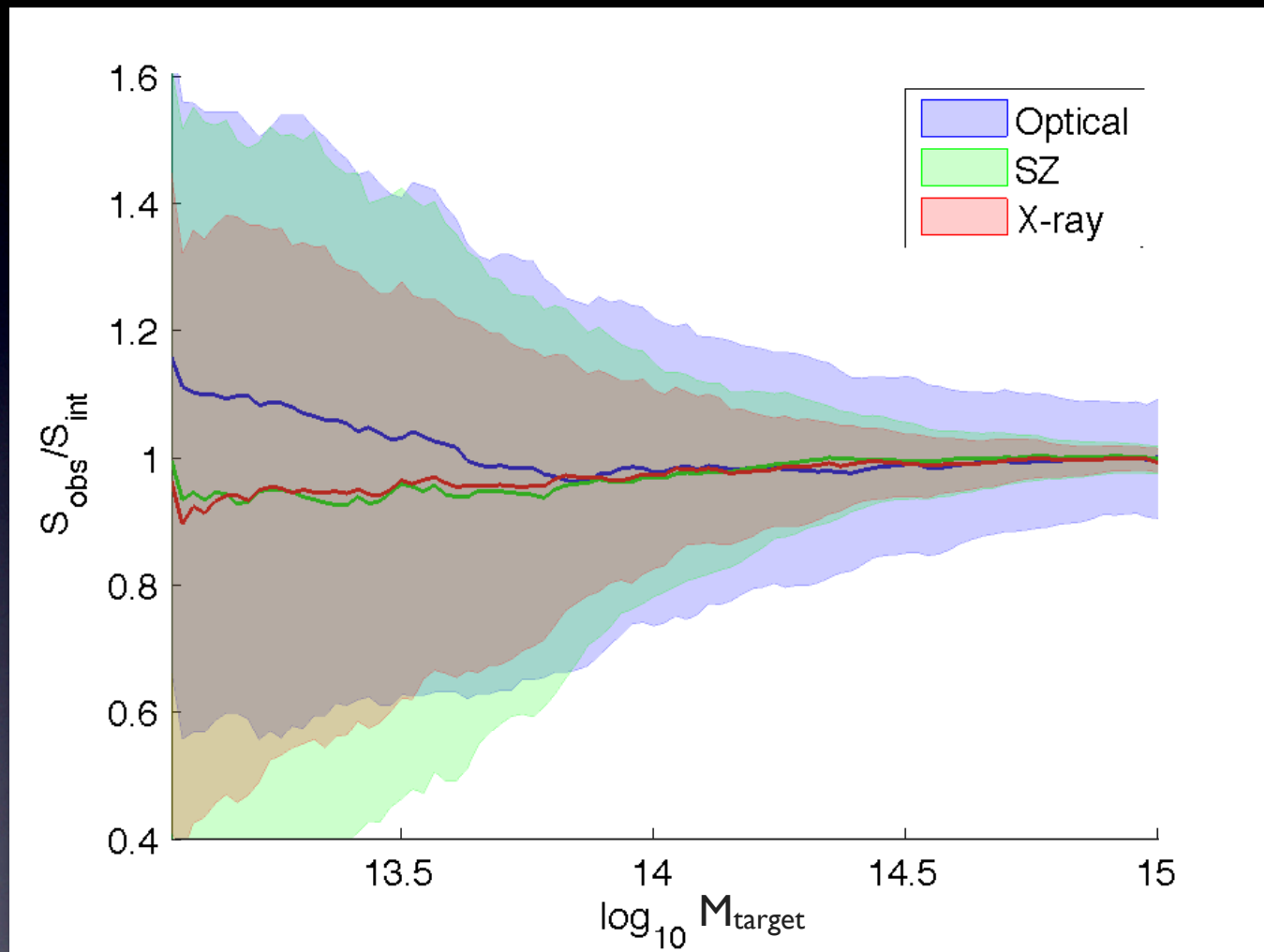
Limiting mass of projected halos



fixed target $z=0.3$

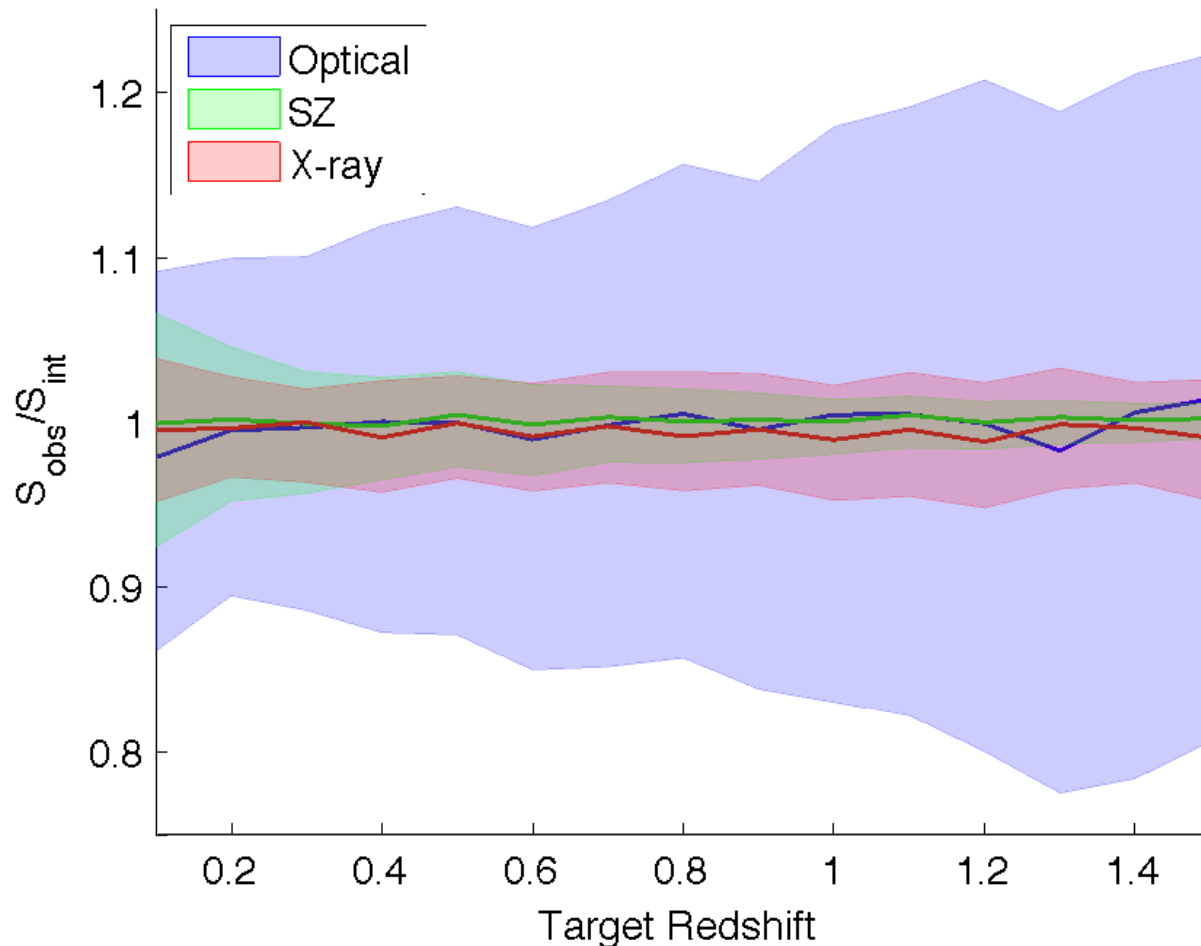
varying target mass

lower masses incur
larger projection



fixed target $z=0.3$

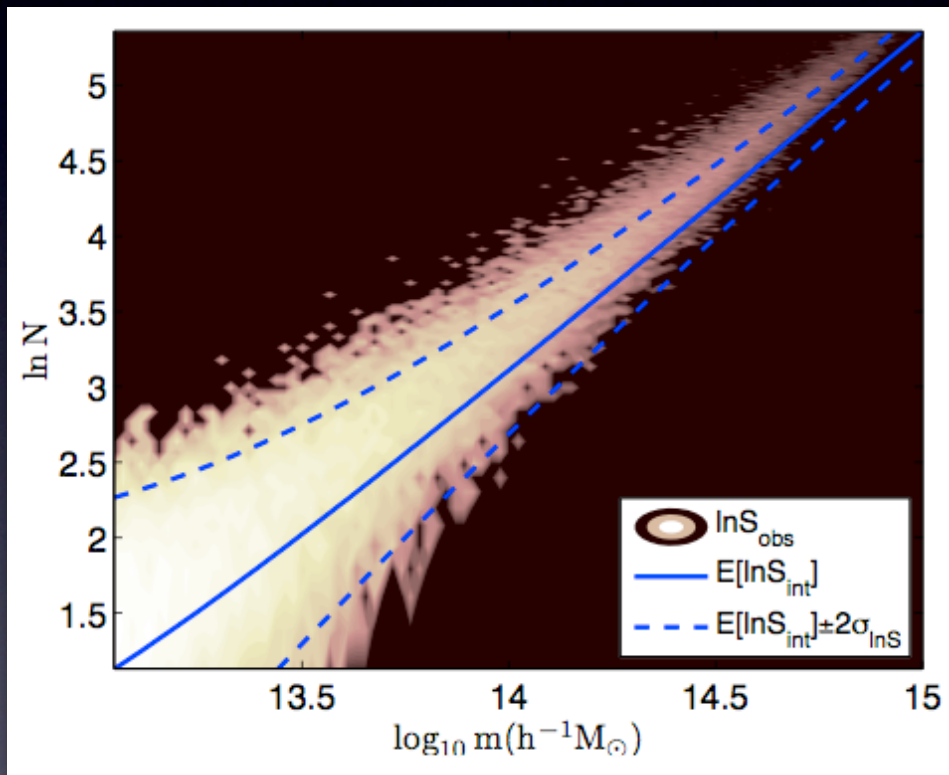
after **local background subtraction** using annulus $\sim(1.7-2.0) \theta_{200}$ surrounding target



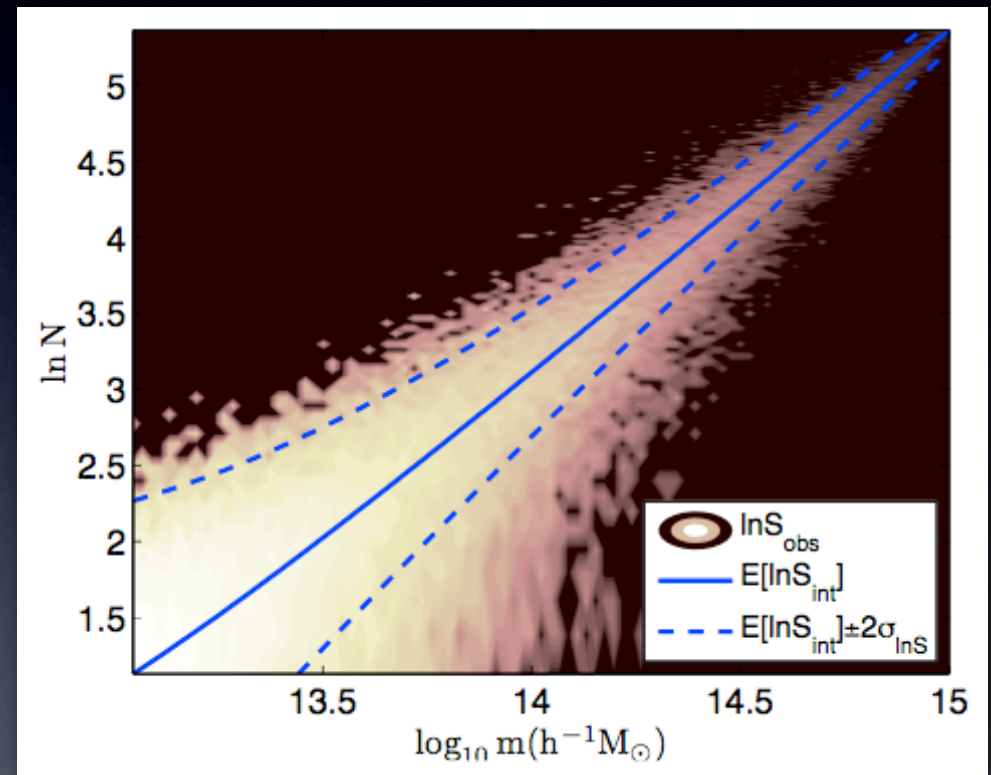
target mass tied to
fixed sky surface
density
(matched to $z=0.3$,
 $10^{14.5}$ Msun halos)

after **local
background
subtraction** using
annulus $\sim(1.7-2.0) \theta_{200}$
surrounding target

before



after



- bias is removed but scatter increases
- covariance with X-ray + SZ is also affected

Synthetic Skies for DES

“mock” catalog :(

“synthetic” catalog :)

DES Simulation Working Group: key personnel



Risa Wechsler, asst. professor (Stanford/SLAC)

- ADDGALS methodology, empirical tuning
- DES catalog production lead



Michael Busha, postdoc (Zurich)

- N-body production + postprocessing
- ADDGALS development and application
- DES catalog production (masking, Data Challenge ingest)



Matt Becker, grad student (Chicago)

- N-body production + postprocessing
- gravitational lensing shear (new Spherical Harmonic Tree code)



Brandon Erickson, grad student (Michigan)

- N-body production + postprocessing
- workflow development for XSEDE/SLAC processing (BCC)



Blind Cosmology Challenge (BCC)

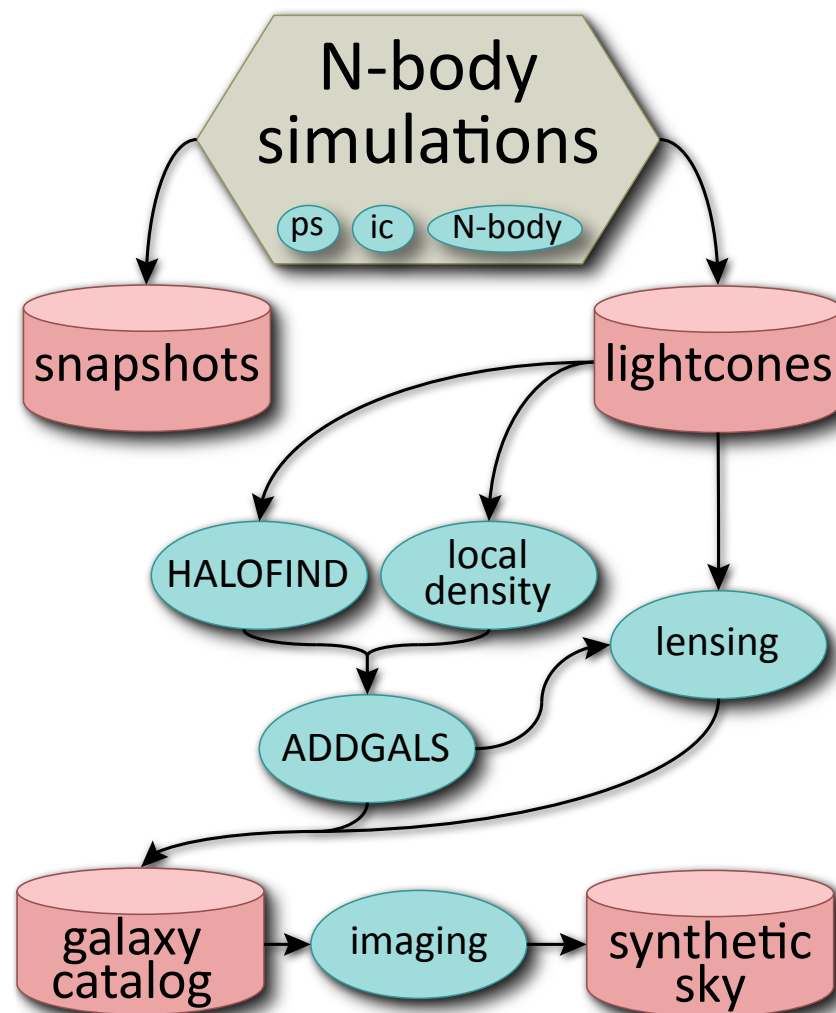


5M cpu-hour XSEDE allocation 2012
ASTI20042, PI: Evrard

To validate science pipelines, DES science teams will analyze synthetic catalogs of ~ 10 different cosmological models, varying DE and other cosmic parameters.

BCC catalogs:

- based on large N-body simulations of dark matter
- post-processed using an empirical approach to link galaxy properties to dark matter structures (*halos*)
- small patch (~ 200 sq deg) of catalog is processed to synthetic imaging based on DECam design, images run through data management pipeline@NCSA (Data Challenge process)



BCC Sky Survey Generation



- 4 nested volumes: 1.0 to 6.0 Gpc/h
 - better match to apparent mag limit of DES
 - + small (0.4 Gpc/h) run to calibrate ADDGALS with SHAM (Sub-Halo Assignment Matching)
- sky survey built from lightcone segments of 1.0-6.0 Gpc/h runs

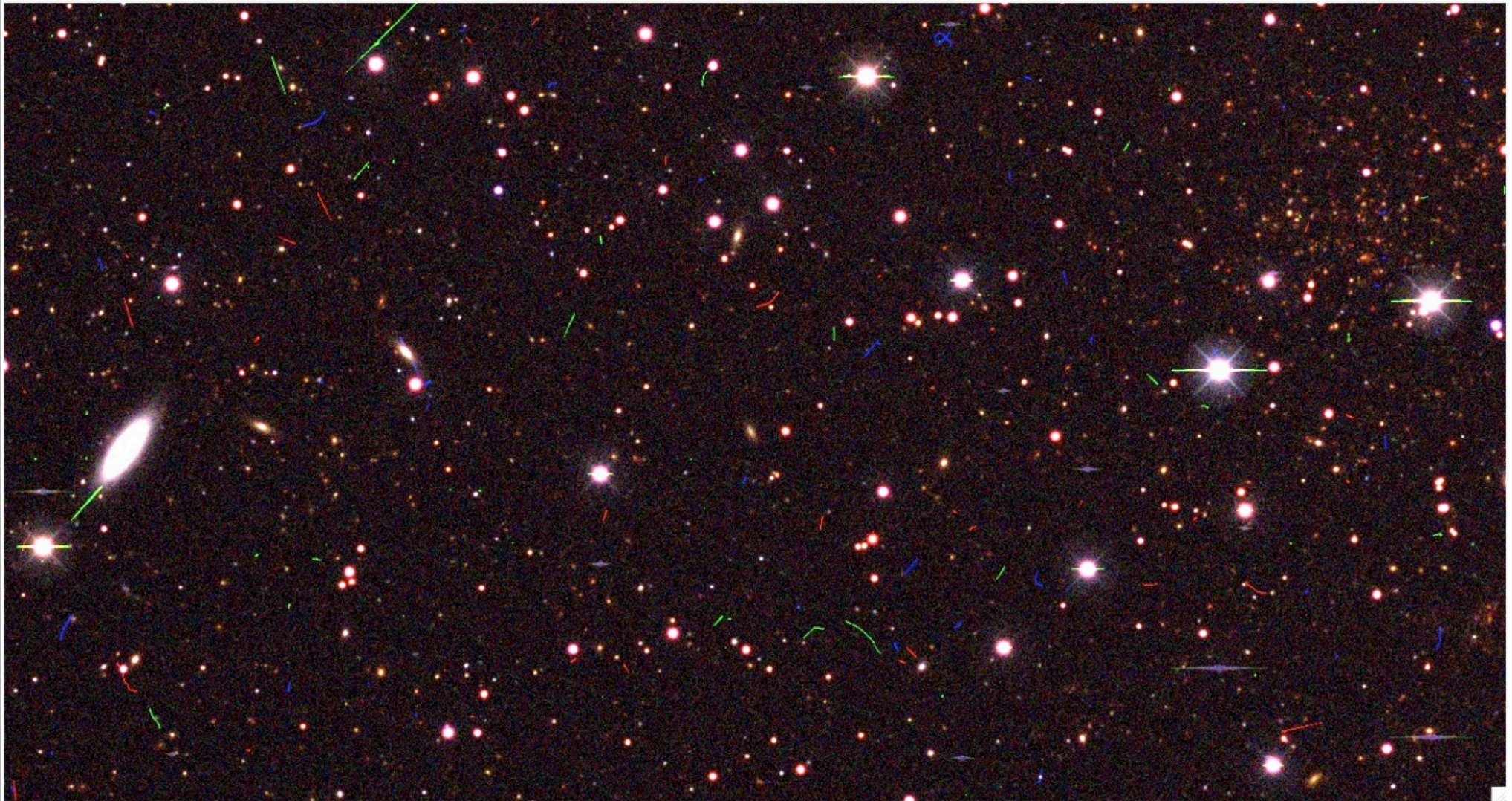
$\Omega_{rmM}, \Omega_B, \Omega_{DE}, \Omega_K, \Omega_\nu, h, \sigma_8, n_s, f_{NL}, w_0, w_a$
{Lb, Np, z_{ini} , randSeed, paths/to/data/products...}

Lb h^{-1} Gpc	Np	$\sim z$	kCPUhr	TB
0.42	1400^3	–	230	25
1.05	1400^3	0.3	50	3
2.60	2048^3	0.9	125	9
4.00	2048^3	2	115	9
6.00	2048^3	6	105	9

BCC synthetic 3'x5' image



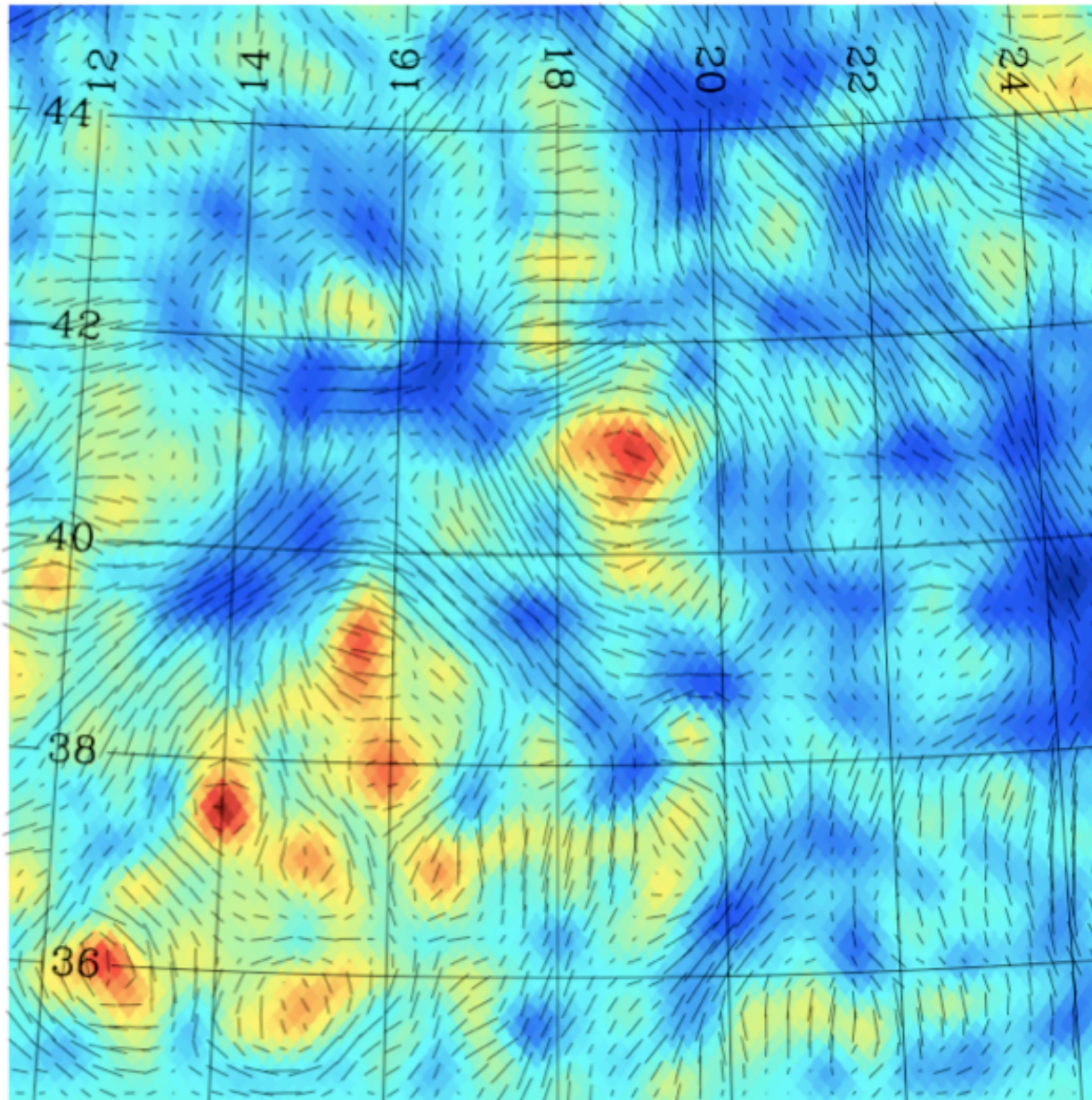
H. Lin (Fermilab)





HEALPix-based map of DC6B 200 deg² convergence and shear fields

DAI
SUI



*Colors indicates
convergence \propto
surface mass
density;
redder \implies
higher density*

*Black “whiskers”
show shear field
due to
gravitational
lensing*

Figure from M. Becker

BCC catalog content



Risa Wechsler, DES Penn Collaboration Mtg, Oct 2011



BCC “observed” information

Available now for v3.02

- RA: Right ascension (lensed).
- DEC: Declination (lensed).
- MAG_ [UGRIZY]: The observed DES magnitudes with photometric errors applied to LMAG.
- MAGERR_ [GRIZY]: Estimated photometric errors for each band.
- EPSILON: Observed ellipticity.
- SIZE: Observed size (FLUX_RADIUS).
- PGAL: Probability that the object is a galaxy.
- PHOTOZ_GAUSSIAN: Estimated photo-z using a gaussian PDF with $\sigma = 0.03/(1+z)$.
- ZCARLOS: Redshift estimate from zCarlos code.
- PZCARLOS: ARRAY of $p(z)$ in bin of $\Delta z = 0.02$.
- ARBORZ: Redshift estimate from ArborZ code.
- ARBORZ_ERR: Redshift errorestimate from ArborZ code.
- PZARBOR: ARRAY of $p(z)$ in bin of $\Delta z = 0.032$.
- ANNZ: Redshift estimate from ANNz code.
- ANNZ_ERR: Redshift error estimate from ANNz code.

+ vista magnitudes

■ Is there additional information we should be providing?

final thoughts...

- transition from scarcity to abundance
 - large N-body simulations are now abundant ($\sim 50k$ SU's per 2048^3 run)
 - gas dynamic/MHD simulations remain scarce ($\sim 1M$ SU's per run)
- large survey projects have specific simulation requirements
 - Simulation WG of DES is first survey-specific group in LSS community
 - prior projects (e.g., Hubble Volume, Millennium, Marenstrum) were simulations done as 'theoretical' investigations, published as such
- Euclid/WFIRST/LSST era
 - LSS simulations as **essential** element of survey data analysis*
 - **methods must evolve to support production of large simulation ensembles**

* science agency policies still adjusting to this perspective

up
bottom
from the
ELECTRONICS

Learn More >

1 2 3

SIMULATE with over 235 tools for nanoelectronics, nanophotonics and more >

RESEARCH & COLLABORATE via groups, question board and more >

TEACH & LEARN with tool-powered curricula, courses, seminars and more >

SHARE & PUBLISH tools and research through our easy upload process

A resource for nanoscience and nanotechnology, nanoHUB.org was created by the NSF-funded Network for Computational Nanotechnology.

Over 230,000 users annually

39 Live Simulation Sessions

[Detailed statistics](#) | [Who's online?](#)